RMZ

MATERIALS and GEOENVIRONMENT

MATERIALI in GEOKOLJE

RMZ – M&G, **Vol. 67**, No. 1
pp. 001–038 (2020)

Ljubljana, March 2020

RMZ – Materials and Geoenvironment
RMZ – Materiali in geookolje
ISSN 1408-7073

Old title/Star naslov
Mining and Metallurgy Quarterly/Rudarsko-metalurški zbornik
ISSN 0035-9645, 1952–1997

Published by/Izdajatelj
Faculty of Natural Sciences and Engineering, University of Ljubljana/
Naravoslovnotehniška fakulteta, Univerza v Ljubljani

Associated Publisher/Soizdajatelj
Institute for Mining, Geotechnology and Environment, Ljubljana/
Inštitut za rudarstvo, geotehnologijo in okolje
Velenje Coal Mine/Premogovnik Velenje
Slovenian Chamber of Engineers/Inženirska zbornica Slovenije

Editorial Address/Naslov uredništva
RMZ – Materials and Geoenvironment
Aškerčeva cesta 12, p. p. 312
1001 Ljubljana, Slovenija
Tel.: +386 (0)1 470 46 10
Fax.: +386 (0)1 470 45 60
E-mail: bostjan.markoli@ntf.uni-lj.si
joze.zarn@ntf.uni-lj.si

Published/Izhajanje
4 issues per year/4 številke letno

Partly funded by Ministry of Education, Science and Sport of Republic of Slovenia./Pri financiranju revije sodeluje Ministrstvo za izobraževanje, znanost in šport Republike Slovenije.

Articles published in Journal "RMZ M&G" are indexed in international secondary periodicals and databases:/Članki, objavljeni v periodični publikaciji „RMZ M&G", so indeksirani v mednarodnih sekundarnih virih: CA SEARCH® – Chemical Abstracts®, METADEX®, GeoRef.

Annual subscription for individuals in Slovenia: 20 EUR, for institutions: 30 EUR. Annual subscription for the rest of the world: 30 EUR, for institutions: 50 EUR/Letna naročnina za posameznike v Sloveniji: 20 EUR, za inštitucije: 30 EUR. Letna naročnina za tujino: 30 EUR, inštitucije: 50 EUR

Transaction account/Tekoči račun
Nova Ljubljanska banka, d. d., Ljubljana: UJP 01100-6030708186

VAT identification number/Davčna številka
24405388

Online Journal/Elektronska revija
https://content.sciendo.com/view/journals/rmzmag/rmzmag-overview.xml?result=4&rskey=iClOT4#

Table of Contents

Kazalo

Historical Review

More than 90 years have passed since the University Ljubljana in Slovenia was founded in 1919. Technical fields were united in the School of Engineering that included the Geologic and Mining Division, while the Metallurgy Division was established only in 1939. Today, the Departments of Geology, Mining and Geotechnology, Materials and Metallurgy are all part of the Faculty of Natural Sciences and Engineering, University of Ljubljana.

Before World War II, the members of the Mining Section together with the Association of Yugoslav Mining and Metallurgy Engineers began to publish the summaries of their research and studies in their technical periodical Rudarski zbornik (Mining Proceedings). Three volumes of Rudarski zbornik (1937, 1938 and 1939) were published. The War interrupted the publication and it was not until 1952 that the first issue of the new journal Rudarsko-metalurški zbornik – RMZ (Mining and Metallurgy Quarterly) was published by the Division of Mining and Metallurgy, University of Ljubljana. Today, the journal is regularly published quarterly. RMZ – M&G is co-issued and co-financed by the Faculty of Natural Sciences and Engineering Ljubljana, the Institute for Mining, Geotechnology and Environment Ljubljana, and the Velenje Coal Mine. In addition, it is partly funded by the Ministry of Education, Science and Sport of Slovenia.

During the meeting of the Advisory and the Editorial Board on May 22, 1998, Rudarsko-metalurški zbornik was renamed into "RMZ – Materials and Geoenvironment (RMZ – Materiali in Geookolje)" or shortly RMZ – M&G. RMZ – M&G is managed by an advisory and international editorial board and is exchanged with other world-known periodicals. All the papers submitted to the RMZ – M&G undergoes the course of the peer-review process.

RMZ – M&G is the only scientific and professional periodical in Slovenia which has been published in the same form for 60 years. It incorporates the scientific and professional topics on geology, mining, geotechnology, materials and metallurgy. In the year 2013, the Editorial Board decided to modernize the journal's format.

A wide range of topics on geosciences are welcome to be published in the RMZ – Materials and Geoenvironment. Research results in geology, hydrogeology, mining, geotechnology, materials, metallurgy, natural and anthropogenic pollution of environment, biogeochemistry are the proposed fields of work which the journal will handle.

Editor-in-Chief

Zgodovinski pregled

Že več kot 90 let je minilo od ustanovitve Univerze v Ljubljani leta 1919. Tehnične stroke so se združile v Tehniški visoki šoli, ki sta jo sestavljala oddelka za geologijo in rudarstvo, medtem ko je bil oddelek za metalurgijo ustanovljen leta 1939. Danes oddelki za geologijo, rudarstvo in geotehnologijo ter materiale in metalurgijo delujejo v sklopu Naravoslovnotehniške fakultete Univerze v Ljubljani.

Pred 2. svetovno vojno so člani rudarske sekcije skupaj z Združenjem jugoslovanskih inženirjev rudarstva in metalurgije začeli izdajanje povzetkov njihovega raziskovalnega dela v Rudarskem zborniku. Izšli so trije letniki zbornika (1937, 1938 in 1939). Vojna je prekinila izdajanje zbornika vse do leta 1952, ko je izšel prvi letnik nove revije Rudarsko-metalurški zbornik – RMZ v izdaji odsekov za rudarstvo in metalurgijo Univerze v Ljubljani. Danes revija izhaja štirikrat letno. RMZ – M&G izdajajo in financirajo Naravoslovnotehniška fakulteta v Ljubljani, Inštitut za rudarstvo, geotehnologijo in okolje ter Premogovnik Velenje. Prav tako izdajo revije financira Ministrstvo za izobraževanje, znanost in šport.

Na seji izdajateljskega sveta in uredniškega odbora je bilo 22. maja 1998 sklenjeno, da se Rudarsko-metalurški zbornik preimenuje v RMZ – Materiali in geookolje (RMZ – Materials and Geoenvironment) ali skrajšano RMZ – M&G. Revijo RMZ – M&G upravljata izdajateljski svet in mednarodni uredniški odbor. Revija je vključena v mednarodno izmenjavo svetovno znanih publikacij. Vsi članki so podvrženi recenzijskemu postopku.

RMZ – M&G je edina strokovno-znanstvena revija v Sloveniji, ki izhaja v nespremenjeni obliki že 60 let. Združuje področja geologije, rudarstva, geotehnologije, materialov in metalurgije. Uredniški odbor je leta 2013 sklenil, da posodobi obliko revije.

Za objavo v reviji RMZ – Materiali in geookolje so dobrodošli tudi prispevki s širokega področja geoznanosti, kot so: geologija, hidrologija, rudarstvo, geotehnologija, materiali, metalurgija, onesnaževanje okolja in biokemija.

Glavni urednik

Received: Mar 11, 2020
Accepted: Mar 13, 2020
DOI: 10.2478/rmzmag-2020-0003

In Memoriam – Assoc. Prof. Dr Ranko Todorović

(30 November 1942–11 December 2019)

The man who has forgotten more than we will be able to learn...

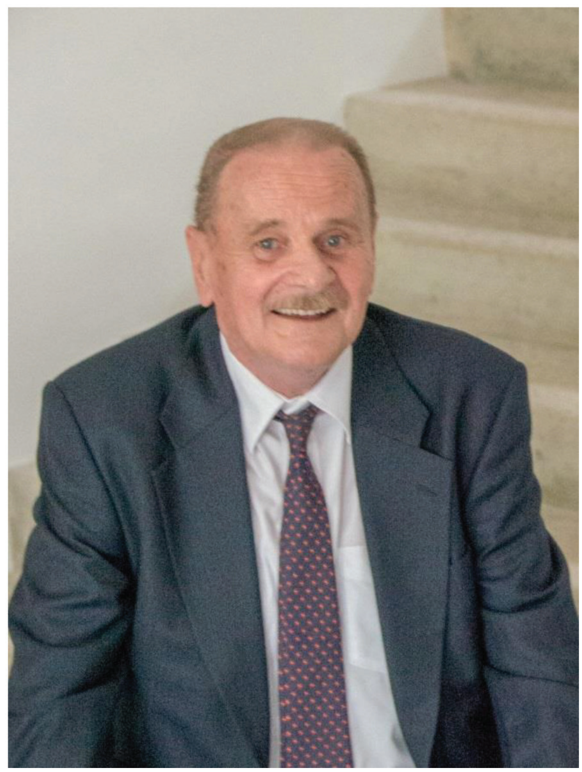

Professor Ranko Todorović left us on December 11, 2019. The mining profession, especially the fields of mining measurements, rock and ground movements and subsidence damages, has lost a world-renowned expert.

He became involved in the mining profession and chose to study mining engineering as a high school student during his summer holidays in France with his uncle, who was the owner of a mine at the time. During his studies, he participated in the educational process as a demonstrator. As a student, he was active in the International Association for the Exchange of Students for Technical Experience (IAESTE), where he organised student exchanges or professional internships. He attended two of these internships himself – at several English coal mines and at an iron mine in Kiruna, Sweden. He completed his mining studies in 1967 with a bachelor thesis in mining measurement, for which he received the University Prešeren Award for Students.

After serving the military, he worked at the Idrija Mercury Mine for 3 years as the Head of the Department of Mining Survey, Slovenia. In October 1971, he began working as an assistant at the Chair for Mine Surveying and Applied Geophysics at the Department of Mining of the then Faculty of Natural Sciences and Technology, University of Ljubljana, where he was to spend most of his career path. From October 1974 to May 1982, he worked as a mining engineer at the Geological Survey of Slovenia, while continuing to work as a contractual associate for the faculty (initially as an assistant and later as an assistant professor), where he was hired full time in July 1982. In December 1986, he completed his PhD in mining damage; the following year, he was first elected to hold the title of Associate Professor of Mining.

Professor Todorović was the Head of the Chair for Mine Surveying and Applied Geophysics for many years. He was also an honorary member of the International Society for Mine Surveying (ISM) and, for several years, he was the President and member of its Committees 1, 2, 3 and 4. He organised several professional symposia in Slovenia and, earlier, in erstwhile Yugoslavia; he had a wide circle of international colleagues, some of whom also became his friends, including Professor Eduard Czubik of the Montanuniversität Leoben, Austria, and Professor Bernard Drzezla of the Silesian University of Technology in Gliwice, Poland.

He wrote and spoke fluently in French, English, German, Slovenian, Serbian and Russian. He would only confirm so much, while we concluded that he also spoke Spanish, Italian, Norwegian, Polish, Czech, Slovak, Macedonian, Ukrainian, and so on; he corrected us that he could only communicate the basics in the mentioned languages. I have listened to many conversations that the late professor conducted in languages that he "can only use the basics" in with native speakers, and I can testify that they have never resorted to using another language.

Professor Todorović always enthusiastically participated in professional discussions and unselfishly assisted his younger colleagues. Many of his ideas first appeared in the works of his doctoral students, but he never allowed these ideas to be presented as his, saying "We did it together". As a professor, he was considered the only one from whom students could receive assistance with any subject they listened to while studying at the Department of Geotechnology, Mining and Environment. Students described him as a man who had forgotten more than they would be able to learn.

Professor Todorović has left behind a library full of professional books, as well as knowledge that will be passed on to new generations by his former students and colleagues at the Department of Geotechnology, Mining and Environment of the Faculty of Natural Sciences and Engineering, University of Ljubljana, Slovenia.

He was an excellent designer of monitoring networks for movements and deformations. He also introduced a time component into the observations – he incorporated dynamic variables, and the measurements were not only a function of the "YXH" coordinates but also of the time coordinate "t", so that the observation points that Professor Todorović adjusted also had the coordinate "t". He was well versed in various statistical methods of submergence. The introduction of the "t" coordinate has been a great help in predicting damage, one of the most difficult practical problems that miners face.

He cooperated with all operating mines in Slovenia (Idrija, Velenje, Trbovlje-Hrastnik, Žirovski vrh) and left behind high-quality networks everywhere, as well as a very high number of the well-predicted consequences of mining. For several years, he was an associate of the Institute of Mining, Geotechnology and Environment; with his knowledge and experience, he was also involved in the construction of the Karawanks Tunnel.

After retiring in 2004, he focused most on enjoying the company of his grandchildren, but he continued to work with the faculty and was always ready to help as a counsellor. He will remain in our fondest memories.

Professor Ranko Todorović will be sincerely missed by his friends and colleagues. We send our heartfelt condolences to his family.

In the name of and in my personal name

Assoc. Prof. Dr Milivoj VULIĆ
Faculty of Natural Sciences and Engineering
University of Ljubljana
Slovenia

Original scientific paper

Received: Mar 11, 2020
Accepted: Mar 13, 2020
DOI: 10.2478/rmzmag-2020-0002

Environmental Impacts of Mixed Aggregates for use in Unbound Layers in Road Construction

Okoljski vplivi mešanih agregatov za uporabo v nevezanih materialih v cestogradnji

Metka Gostečnik[1,2], Predrag Šinik[1], Ana Mladenovič[3], Janez Ščančar[2,4], Radmila Milačič[2,4,*]

[1] Ekomineral d.o.o., Savinjska cesta 25, 3310 Žalec, Slovenia
[2] Jožef Stefan International Postgraduate School, Jamova 39, 1000 Ljubljana, Slovenia
[3] Department of Materials, Slovenian National Building and Civil Engineering Institute, Dimičeva 12, 1000 Ljubljana, Slovenia
[4] Department of Environmental Sciences, Jožef Stefan Institute, Jamova 39, 1000 Ljubljana, Slovenia
* radmila.milacic@ijs.si

Abstract

During carbon steel manufacturing, large amounts of electric arc furnace (EAF) slag are generated. EAF slag, if properly treated and processed into aggregate, is an alternative source of high-quality material, which can substitute the use of natural aggregates in most demanding applications in the construction sector, mostly for wearing asphalt courses. In this screening process of high-quality aggregates, a side material with grain size 0/32 mm is also produced, which can be used as an aggregate for unbound layers in road construction. In this study, the environmental impacts of slag aggregate (fraction 0/32 mm) were evaluated in mixed natural/slag aggregates. Different mixtures of natural/slag aggregates were prepared from aged (28 days) and fresh slag, and their environmental impacts were evaluated using leaching tests. It was shown that among the elements, chromium (Cr) was leached from some mixed aggregates in quantities that exceeded the criterion for inert waste. The data from the present investigation revealed that mixed aggregates, prepared from aged slag (fraction 0/32 mm) and natural stone in the ratio 10/90, are environmentally acceptable and can be safely used in unbound materials for road construction.

Keywords: electric arc furnace slag, natural aggregate, mixed aggregates, environmental impacts, unbound materials for road construction.

Povzetek

Med proizvodnjo ogljičnega jekla v elektroobločnih pečeh nastajajo velike količine žlindre. Pravilno obdelana in predelana žlindra je odličen material, ki lahko uspešno nadomesti naravne agregate. Pred uporabo se žlindra stara, drobi in separira v agregate različnih frakcij, ki se uporabljajo v gradbeništvu, predvsem kot visokokakovosten agregat v obrabnih asfaltnih plasteh. Med separiranjem nastaja tudi agregat zrnavosti 0/32 mm, ki ni primeren za uporabo v asfaltnih plasteh, temveč se uporablja za nevezane nosilne plasti v cestogradnji. V našem delu smo preučili okoljske vplive mešanega agregata (frakcija 0/32 mm) žlindre in naravnega agregata za njegovo uporabo v nevezanih materialih v cestogradnji. Pripravili smo različne mešanice iz naravnega agregata in agregata iz žlindre. Uporabili smo svežo in starano (28 dni) žlindro ter ocenili okoljske vplive pripravljenih mešanic z izlužitvenimi testi. Rezultati naše raziskave so pokazali, da se iz nekaterih pripravljenih mešanic lahko izlužuje element krom (Cr) v količinah, ki presegajo mejno vrednost za inertne odpadke. Kot nevezane materiale v cestogradnji varno lahko uporabimo agregate, ki smo jih pripravili iz agregata iz starane žlindre (frakcija 0–32 mm) in naravnega agregata v razmerju med 10/90.

Ključne besede: žlindra iz elektroobločne peči, naravni agregat, mešani agregati, okoljski vplivi, nevezani materiali v cestogradnji.

Introduction

Industrial wastes or by-products are increasingly being used as alternative materials that successfully substitute natural raw materials. Recycling and use of these materials lead to the preservation of natural resources, significant reduction of landfill load and protection of the environment [1]. Recycling of waste materials is in line with the main objectives of green building, i.e. application of processes that are environmentally responsible and resource efficient. The latter goals are strongly supported by the Directive 2018/851/ES on waste [2] and Construction Products Regulation No. 305/2011 [3]. During steel manufacture, huge amounts of waste materials, such as electric arc furnace (EAF) slag, ladle slag and EAF filter dust, are produced. In the Štore Steel plant, Slovenia, the annual steel production is about 150,000 tonnes. Approximately 20,000 tons of EAF slag, 2,000 tons of ladle slag and 2,500 tons of EAF dust are generated as waste per year [4].

During the production of steel in an EAF, scrap metal or metallised ore, or both, are melted along with lime in refractory lined vessels. Throughout the melting process, oxygen is injected into the molten steel, which oxidises a part of metallic Fe and alloying components (e.g. Mn, Ni, Cr, Mo, V), as well as the impurities in steel scrap (e.g. Al, Si, Mn, P and C). The EAF steel slag is poured from the furnace in a molten state at the end of the process. About 15–20% of EAF slag occurs per equivalent unit of steel. The principal components of EAF steel slag are calcium silicates and ferrites, together with oxides and compounds of iron, magnesium, manganese and alumina, which together make up 95% of the slag [5]. The main minerals in slag are wustite, dicalcium silicate, tricalcium silicate and brownmillerite; and the accessory minerals can be spinel, barite, CaO and MgO. Both of the latter components are unstable. In the presence of moisture, they transform into $Mg(OH)_2$ and/or $Ca(OH)_2$, which occupy a larger volume than the primary components. The result is swelling of the composite into which the slag has been placed. The slag must therefore be "aged" long enough for the CaO and MgO to be transformed into stable forms. Slow, controlled cooling also enables this material to develop a microtexture, which ensures long-term toughness and roughness and is comparable with the porphyric texture of volcanic rocks.

EAF slag is highly durable and is, in terms of its physico-mechanical characteristics, comparable to high-quality natural rocks. Due to its excellent physical and mechanical properties, it can be used as an alternative material that successfully replaces natural aggregates. Hence, the greatest potential for recycling and use of steel slag is in the construction sector [6–9]. EAF slag aggregate is used in different types of concrete [9–13], in sub-base layer constructions [14, 15], and especially in asphalt mixes [6, 7, 16–18]. Other EAF slag applications include water and wastewater treatment [9], as well as usage in synthesis of alkali-activated materials [19].

The use of materials that contain industrial waste and/or by-products is possible when such materials possess appropriate technical characteristics [15, 20–23] and are environmentally acceptable [20–24]. For evaluation of the environmental impacts of raw materials and final products, the extent of leaching of contaminants is estimated by applying different leaching tests, e.g. the European test method for leaching of aggregates (Slovenian Institute for Standardisation [SIST] EN 1744-3) [25] and the compliance test for the leaching of granular waste materials and sludges (SIST EN 12457-4) [26]. In these leaching tests, shaking of the solid material with water (a liquid-to-solid ratio of 10 L/kg) is performed over 24 h.

The EAF slag, which is generated during the metallurgical process of carbon steel production in Štore Steel (waste classification no.: 10 02 02), is first subjected to stabilisation by ageing. For this purpose, a process of slow cooling, wetting with water and temporary storage for a period of 28 days (ageing) is carried out. Before final crushing and screening of the aggregate, iron is extracted by magnetic separation. The 32/300 mm fraction is mostly used for unbound layers, the 32/63 mm fraction particles for railway ballast and the 2/4 mm, 4/8 mm and 8/11 mm fractions for asphalt mixes. During these screenings, an additional fraction (0/32 mm) is also formed, which is the material for unbound layers in road construction. Therefore, the aim of the present study was to evaluate the potential use of the mixed aggregate (0/32 mm) from the EAF slag aggregate and natural aggregate as the unbound material for road construction from the environmental point of view. Different mixed aggregates were prepared and their environmental impacts were estimated by applying leaching tests.

Materials and Methods

Reagents

Merck (Darmstadt, Germany) suprapur acids and Milli-Q water (Direct-Q 5 Ultrapure water system; Millipore, Watertown, MA, USA) were used for the preparation of samples and standard solutions. Certipur inductively coupled plasma spectroscopy (ICP) multi-element standard solution IV (1,000 ± 5 mg/L in 5% HNO_3) and single stock standard solution of Hg (1,000 ± 5 mg/L in 5% HCl), both purchased from Merck, were used for the preparation of calibration curves in ICP–mass spectroscopy (MS) determinations. To control the stability of ICP–MS, Merck Ge, Rh, Sc and In (1,000 ± 2 mg/L in 5% HNO_3) were used as internal standards. The reagents for spectrophotometry were obtained from Hach Lange GmbH (Düsseldorf, Germany). Cellulose nitrate membrane filters (0.45 mm; Sartorius, Gottingen, Germany) were used for filtration. The certified reference material CRM 320R (trace elements in river sediment; Community Bureau of Reference, Geel, Belgium), the standard reference material SPS-SW1 (reference material for measurement of elements in surface waters; obtained from Spectrapure Standards, Oslo, Norway) and reference material Anions – Whole Volume (purchased from Merck) were used to check the accuracy of the analytical procedures.

Apparatus

The concentrations of elements in the leachates of natural aggregate, EAF slag aggregate and mixed aggregates were determined by ICP–MS on an Agilent 7700´ spectrometer (Agilent Technologies, Tokyo, Japan). The ICP–MS operating parameters are presented in Table 1.

Table 1. *ICP–MS operating parameters for determination of element concentrations*

Parameter	Type/value	Helium mode	No gas mode
Sample introduction			
Nebuliser	Mira Mist		
Spray chamber	Scott		
Skimmer and sampler	Ni		
Plasma conditions			
Forward power	1,550 W		
Plasma gas flow	15.0 L/min		
Carrier gas flow		1.05 L/min	0.75 L/min
Dilution gas flow		0.10 L/min	0.45 L/min
He gas flow		4.5 mL/min	
Quadrupole (QP) bias		–15 V	–3.6 V
Octapole (Oct) bias		–18 V	–8.0 V
Cell entrance		–40 V	–40 V
Cell exit		–60 V	–50 V
Deflect		–2.2 V	13.4 V
Plate bias		–60 V	–40 V
Sample uptake rate	0.3 mL/min		
Data acquisition parameters			
Isotopes monitored		^{52}Cr, ^{60}Ni, ^{63}Cu, ^{66}Zn, ^{75}As, ^{78}Se, ^{95}Mo	^{111}Cd, ^{121}Sb, ^{137}Ba, ^{201}Hg, ^{208}Pb
Isotopes of internal standards		^{45}Sc, ^{72}Ge, ^{103}Rh, ^{115}In	^{45}Sc, ^{72}Ge, ^{103}Rh, ^{115}In

The contents of chlorides, sulphates and fluorides were determined on the DR 3900 portable spectrophotometer (Hach, Manchester, Great Britain). The MARS 6 Microwave System (CEM Corporation; Matthews, NC, USA) was used for digestion of the slag samples. The WTW 330 pH meter (WTW, Weilheim, Germany) was used to determine the pH. The Mettler AE 163 (Mettler Toledo, Zürich, Switzerland) analytical balance was used for weighing.

Samples

The EAF slag samples from different batches were obtained from Štore Steel Company, Štore, Slovenia. After ageing of the slag and production of aggregate fractions, the 0/32 mm fractions from fresh and aged slags (time of ageing: 28 days) were used in the present study. Natural aggregate (dolomite) was obtained from Andraž Quarry, Slovenia. Mixed aggregates of different natural-to-slag ratios were prepared from fresh and aged slags.

Sample preparation

To determine the total content of elements in the slag and aggregate samples, about 0.25 g of sample was subjected to microwave-assisted digestion, using a mixture of nitric, hydrochloric and hydrofluoric acids [27], and the concentrations of the elements in the digested samples were determined by ICP-MS.

The extent of leaching of selected elements and anions from bulk natural aggregates, bulk slag aggregates and bulk mixed aggregates of different ratios was evaluated by the preparation of aqueous leachates (a liquid-to-solid ratio of 10 L/kg), following the SIST EN 1744-3 [25] test method for leaching of aggregates and the SIST EN 12457-4 [26] compliance test for the leaching of granular waste materials and sludges. The concentrations of elements and anions in the aqueous leachates were determined by ICP-MS and spectrophotometry, respectively. The results are presented on a dry mass basis.

Results and Discussion

Quality control of the analytical data

The accuracy of determination of the total metal concentrations in the EAF slag aggregate was checked by analysis of CRM 320R, the total metal concentrations in the leachates were analysed by the SPS-SW1 quality control method and determination of anions was done by analysing the reference material Anions – Whole Volume. The results are presented in Tables 2–4.

Table 2. *Concentrations of elements in certified reference material CRM 320R (Trace Elements in River Sediment) determined by ICP-MS after microwave-assisted digestion*

Element	Certified (mg/kg)	Determined (mg/kg)
Fe	25,700 ± 1,300	24,350 ± 700
Mn	910 ± 50	940 ± 30
Cr	59 ± 4	61 ± 2

Note: The results represent the mean concentration from two parallel samples.

Table 3. *Concentrations of elements in standard reference material SPS-SW1 (reference material for measurements of elements in surface waters) determined by ICP-MS*

Parameter	Certified concentration (mg/L)	Determined concentration (mg/L)
As	10.0 ± 0.1	10.4 ± 0.3
Ba	50 ± 1	52 ± 1
Cd	0.50 ± 0.01	0.48 ± 0.01
Total Cr	2.00 ± 0.02	1.97 ± 0.02
Cu	20 ± 1	19.6 ± 0.3
Mo	10.0 ± 0.1	9.8 ± 0.2
Ni	10.0 ± 0.1	10.2 ± 0.3
Pb	5.0 ± 0.1	4.91 ± 0.01
Se	2.00 ± 0.02	2.03 ± 0.02
Zn	20[a]	21.0 ± 0.2

[a] *Informative value.*

Notes: The results represent the mean concentration from two parallel samples.

Table 4. *Concentrations of chlorides, fluorides and sulphates in reference material Anions – Whole Volume determined by spectrophotometry*

Parameter	Certified concentration (mg/L)	Determined concentration (mg/L)
Chlorides	95.0 ± 9.50	92.5 ± 5.0
Fluorides	1.17 ± 0.117	1.14 ± 0.06
Sulphates	44.3 ± 4.43	42.5 ± 2.0

Note: The results represent the mean concentration from two parallel samples.

Data from Tables 2–4 show good agreement between the determined and certified values (the agreement between the results is better than ±5%), which confirmed the accuracy of the applied analytical procedures for the determination of (a) elements in the EAF slag aggregate and (b) elements and anions in aqueous leachate samples.

Chemical composition of the EAF slag

The chemical composition of the EAF slag aggregate may differ according to the additives used in steel production. The concentration ranges of the main components in the EAF slag analysed are presented in Table 5. During EAF slag processing, elemental oxides are formed. Therefore, concentrations of the measured elements in Table 5 are expressed in the form of their corresponding oxides. Results showed that the content of P_2O_5 and V_2O_5 was <1%, while oxides of other elements (Mo, Ba, Ni and Zn) were found in trace amounts.

Table 5. *Concentration ranges of elemental oxides in EAF slag aggregate samples (0–32 mm) determined by ICP-MS after microwave-assisted digestion*

Parameter	Concentration (%)
FeO and Fe_2O_3	33–46
CaO	20–35
SiO_2	10–20
MgO	3–13
Al_2O_3	3–6
Mn_2O_5	3–5
Cr_2O_3	1–3

Notes: Measurement uncertainty is better than ±3%. Results represent concentration ranges obtained from five EAF slag samples.

As can be seen from the data of Table 5, the main components in the EAF slag are oxides of Fe, Ca, Si and Mg, whereas oxides of Al, Mn and Cr in general occur in concentrations <5%.

Environmental impacts of mixed aggregates from natural and EAF slag aggregates

In order to evaluate the environmental impacts of the mixed aggregates prepared from natural aggregate and EAF slag aggregate, leachates of bulk aggregates were prepared according to relevant test methods (a liquid-to-solid ratio of 10 L/kg) [25, 26]. First, natural aggregate from the Andraž Quarry, aged EAF slag aggregate (0/32 mm) and mixed aggregate containing aged slag aggregate (natural aggregate-to-EAF slag aggregate ratio 30/70) were examined. Concentrations of elements and anions in leachates were determined by ICP-MS and spectrophotometry, respectively. The measured parameters were selected based on the legislative requirements for inert waste [28]. Aggregates used in the unbound materials for road construction and earthwork structures are generally compacted at optimum moisture content in order to ensure maximum density and bearing capacity of the final product. In order to evaluate the environmental impacts of such aggregates, the worst-case scenario was considered. Therefore, the leaching procedure was not performed on the compacted aggregate sample but rather on the bulk sample without any pre-treatment. The results of these experiments, along with the concentration limits for inert waste [28], are presented in Table 6.

As evident, the leaching of elements and anions from natural aggregate is below the instrumental limits of detection for all measured parameters. Due to the presence of soluble $Ca(OH)_2$, which is formed after reaction of CaO with water, the pH values of EAF slag aggregate and mixed natural/EAF slag aggregate are high (pH 12.5 and 12, respectively). As a consequence of the high pH, most of the elements in the aqueous leachates are precipitated. Hence, their concentrations in the leachates are very low, in general, far below the concentration limits for inert waste (Table 6). Attention should be paid to Cr, the concentration of which exceeded the concentration limit of 0.5 mg/kg for inert waste in EAF slag aggregate and in mixed natural/EAF slag aggregates. Cr in EAF slag aggregate is present in the highly insoluble chromite mineral in its trivalent oxidation state. However, at high pH, traces of trivalent Cr are solubilised as the $Cr(OH)_4^-$ complex. Although only a negligible amount, about 0.01% of the total Cr content in the EAF slag aggregate is leached with water; the solubilised Cr(III) is, under the highly alkaline conditions, almost completely oxidised to hazardous Cr(VI) by the presence of dissolved oxygen. As an oxyanion, chromate (CrO_4^{2-}), under alkaline pH values, is a highly mobile and

Table 6. *Concentrations of As, Ba, Cd, Cr, Cu, Hg, Mo, Ni, Pb, Sb, Se and Zn in aqueous leachates (a liquid-to-solid ratio of 10 L/kg) of bulk natural aggregate, bulk aged EAF slag aggregate (0–32 mm) and bulk mixed aggregate from the aged EAF slag aggregate (natural aggregate-to-slag aggregate ratio 30/70) determined by ICP-MS and the content of chlorides, fluorides and sulphates determined by spectrophotometry*

Parameter	Natural aggregate	EAF slag aggregate (0–30 mm)	Mixed aggregate (natural aggregate-to-slag aggregate ratio 30/70)	Concentration limits for inert waste*
As (mg/kg)	<0.001	<0.001	<0.001	0.5
Ba (mg/kg)	<0.02	14	2.2	20
Cd (mg/kg)	<0.002	<0.002	<0.002	0.04
Total Cr (mg/kg)	<0.002	1.4	0.95	0.5
Cu (mg/kg)	<0.001	<0.001	<0.001	2
Hg (mg/kg)	<0.001	<0.001	<0.001	0.01
Mo (mg/kg)	<0.002	0.26	0.24	0.5
Ni (mg/kg)	<0.002	<0.002	<0.002	0.4
Pb (mg/kg)	<0.005	0.45	0.15	0.5
Sb (mg/kg)	<0.001	0.08	0.02	0.06
Se (mg/kg)	<0.003	<0.003	<0.003	0.1
Zn (mg/kg)	<0.005	1.95	0.2	4
Chlorides (mg/kg)	<7	<7	<7	800
Fluorides (mg/kg)	<1	4.59	<1	10
Sulphates (mg/kg)	<10	19.5	<10	1000
pH	8.7	12.5	12.0	/

**Decree on waste (2015): Official Gazette of Republic Slovenia RS, No. 37/15 and No. 69/15.*
Notes: The results represent the mean concentration obtained from two parallel analyses of leachate. Measurement uncertainty for ICP-MS is better than ±3% and, for spectrophotometry, it is ±5%.

highly stable species [23]. Similarly to Cr, Mo also forms the oxyanion molybdate (MoO_4^{2-}), and thus, its leaching from slag aggregates is favourable at high pH values. Leaching of chlorides, fluorides and sulphates from mixed aggregates does not represent any environmental burden.

In the following experiments, mixed aggregates from stone and cured EAF slag of the same batch were prepared in different stone–to-EAF slag ratios. Based on the data from Table 6, only Cr and Mo were measured in the aqueous leachates (Figure 1).

It can be seen that Cr and Mo concentrations in the leachates decrease with higher natural aggregate-to-slag aggregate ratio in the mixed aggregate. As expected, the pH also gradually decreased from pH 12 to pH 10. At natural aggregate-to-slag aggregate ratio 30/70 and 90/10, about 0.25 and 0.05 mg/kg of Mo, respectively is leached from the mixed aggregate. These concentrations are lower than the legislative requirements for inert waste

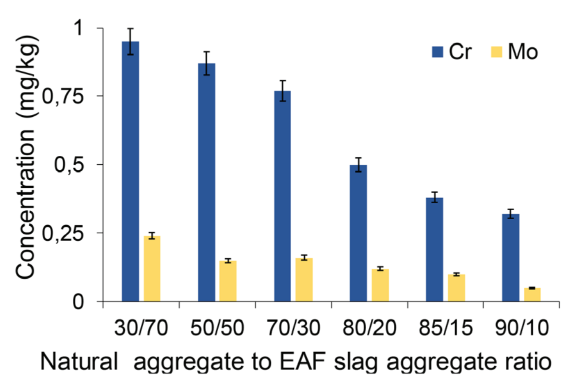

Figure 1. *Concentrations of Cr and Mo in aqueous leachates (a liquid-to-solid ratio of 10 L/kg) of bulk mixed aggregates from aged EAF slag aggregate of the same batch, applying different natural aggregate-to-slag aggregate ratios. Notes: Bars represent mean Cr and Mo concentrations determined by ICP-MS, while the error bars indicate the minimum and maximum concentrations from two parallel determinations in the leachate by ICP-MS.*

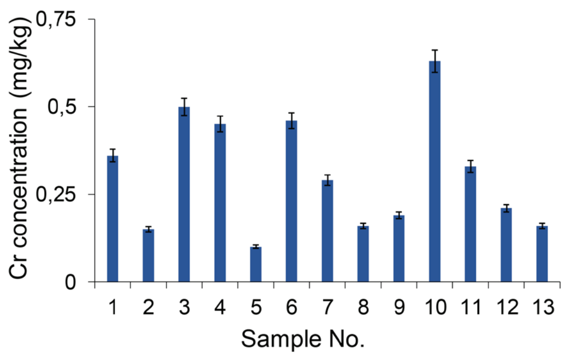

Figure 2. *Concentrations of Cr in aqueous leachates (a liquid-to-solid ratio of 10 L/kg) of bulk mixed aggregates from aged EAF slag of different slag batches, applying natural aggregate-to-slag aggregate ratio 90/10. Notes: Bars represent mean Cr concentrations determined by ICP-MS, while the error bars indicate the minimum and maximum concentrations from two parallel determinations in the leachate by ICP-MS.*

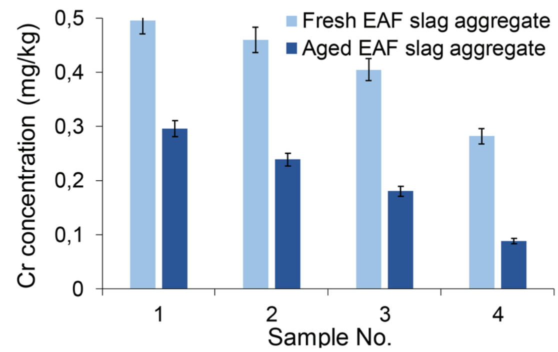

Figure 3. *Concentrations of Cr in aqueous leachates (a liquid-to-solid ratio of 10 L/kg) of bulk mixed aggregates from fresh and aged EAF slags of different slag batches, applying natural aggregate-to-slag aggregate ratio 90/10. Notes: Bars represent mean Cr concentrations determined by ICP-MS, while the error bars indicate the minimum and maximum concentrations from two parallel determinations in the leachate by ICP-MS.*

(0.5 mg/kg Mo) [28]. Cr concentration in the leachate at natural aggregate-to-slag aggregate ratio 30/70 is 0.95 mg/kg and gradually decreases with decrease in the amount of slag aggregate in the mixed aggregate. A concentration that is below the limit for inert waste (0.5 mg/kg Cr) [28] is reached at ratio 85/15.

In order to evaluate the variability of Cr leaching from mixed aggregates, aged slag aggregate from different batches was used for the preparation of mixed aggregates, applying natural aggregate-to-slag aggregate ratio 90/10. These results are presented in Figure 2.

The pH values of the leachates in the samples from Figure 2 were around 10. As evident from the data of Figure 2, the leaching of Cr from 13 mixed aggregates ranged from 0.1 mg/kg up to 0.65 mg/kg. Only two samples exceeded the maximal legislative value set for inert waste. High variability in leached Cr concentrations in the aggregates prepared from aged EAF slag at the same natural aggregate-to-slag aggregate ratio (90/10), with constant pH (10), but from different slag aggregate batches, indicates the high variability of Cr content in the slag aggregate samples from different batches. Cr content in the EAF slag aggregate is related to different compositions of Cr in steel.

Finally, the influence of EAF slag ageing on leaching of Cr from mixed aggregates was estimated. For this purpose, mixed aggregates from four different batches were prepared from fresh and aged EAF slag aggregates, applying natural aggregate-to-slag aggregate ratio 90/10. The results of this experiment are shown in Figure 3.

The pH of the leachates investigated was around 10. The data in Figure 3 demonstrate that, as a consequence of variable Cr content in different slag batches, leached Cr concentrations varied significantly. The ageing of EAF slag, which stabilises its mineralogical phases, results in lower leachability of Cr. Leaching of Cr from mixed aggregates made of aged EAF slag aggregate is 30–60% lower than that of aggregates prepared from fresh slag aggregate from the same batch. It is further evident that Cr leaching from mixed aggregates made of aged EAF slag aggregate (natural aggregate-to-slag aggregate ratio 90/10) from different EAF slag aggregate batches did not exceed 0.3 mg/kg.

Conclusions

The results from the present study revealed that in bulk mixed aggregates (0/32 mm), made of dolomite natural aggregate and EAF slag aggregate, only Cr, among all elements and anions investigated, may exceed the concentration limit for inert waste (0.5 mg/kg Cr). To find the conditions for safe use of mixed aggregates from natural aggregate and EAF slag aggregate, leaching of Cr from samples with different natural aggregate-to-EAF slag aggregate ratios was studied, applying fresh and aged (28 days) EAF slag aggregate from different batches. High pH of mixed aggregates (pH 10–12) enabled the leaching of Cr in the form of oxyanion chromate. Due to variable Cr content in the EAF slag aggregate from different batches, which is related to the composition of steel (different amounts of Cr added in the process to obtain the steel of desired properties), the extent of Cr leaching from mixed aggregates varied significantly. Leaching of Cr from mixed aggregates made from aged EAF slag aggregate was 30–60% lower than that from fresh EAF slag aggregate. Data of the present investigation demonstrated that mixed aggregates prepared from natural aggregate and EAF slag aggregate may be safely used in unbound materials for road construction if aged slag is used for preparation of mixed aggregates at natural aggregate-to-EAF slag aggregate ratio 90/10. The safe reuse of EAF slag leads to the protection of the environment and preservation of natural resources.

Acknowledgements

This work was supported by the Ministry of Education, Science and Sport, the Republic of Slovenia, by co-financing the doctoral studies of Metka Gostečnik at the Jožef Stefan International Postgraduate School (contract number C3330-16-500190). We also acknowledge the financial support received from the Slovenian Research Agency (ARRS) (programme groups P2-0273 and P1-0143).

References

[1] Banaitė, D., Tamošiūnienė, R. (2016): Sustainable development: the circular economy indicators' selection model. *Journal of Security and Sustainability Issues*, 6(2), http://dx.doi.org/10.9770/jssi.2016.6.2(10).

[2] Regulation (EU) No 305/2011 of the European parliament and of the council, of 9 March 2011, Official Journal of the European Union, 4.4.2011.

[3] Official Journal of the European Union. (2011). Regulation (EU) No 305/2011 of the European parliament and of the council laying down harmonised conditions for the marketing of construction products and repealing Council Directive 89/106/EEC, 88, pp. 5–43.

[4] ARSO annual report (2019): *The type and quantity of waste generated in manufacturing and service activities and the ways of managing* (2018), https://www.arso.gov.si/varstvo%20okolja/odpadki/poro%c4%8dila%20in%20publikacije/. Last assessed march 2020.

[5] Yildirim, I., Prezzi, M. (2011): Chemical, mineralogical, and morphological properties of steel slag. *Advances in Civil Engineering*, pp. 1–13, doi:10.1155/2011/463638.

[6] Milačič, R., Zuliani, T., Oblak, T., Mladenovič, A., Ščančar, J. (2011): Environmental impacts of asphalt mixes with electric arc furnace steel slag. *Journal of Environmental Quality*, 40, pp. 115–1161, doi:10.2134/jeq2010.0516.

[7] Oblak, T., Ščančar, J., Vahčič, M., Zuliani, T., Mladenovič, A., Milačič, R. (2011): Environmental impacts of asphalt and cement composites with addition of EAF dust. *RMZ - Materials and Geoenvironment*, 58(2), pp. 181–192.

[8] National Slag Association, Steel slag: A premier construction aggregate, Assessed on March 2020, from http://www.acobrasil.org.br/siderurgiaemfoco/CCABrasil/NSA%20Steel%20Furnace%20Brochure.pdf. Last assessed March 2020.

[9] Lim, J.W., Chew, L.H., Choong, T.S.Y., Tezara, C., Yazdi, M.H. (2016): Overview of Steel Slag Application and Utilization, MATEC Web of Conferences 74, 00026, pp. 1–5, DOI: 10.1051/matecconf/20167400026.

[10] Arribas, I., Vegas, J., San-José, J., Manso, J.M. (2014): Durability studies on steelmaking slag concretes. *Materials & Design*, 63, pp. 168–176, https://doi.org/10.1016/j.matdes.2014.06.002.

[11] Arribas, I., Santamaría, A., Ruiz, E., Ortega-López, Manso, J.M. (2015): Electric arc furnace slag and its use in hydraulic concrete. *Construction and Building Materials*, 15, pp. 68–79, https://doi.org/10.1016/j.conbuildmat.2015.05.003.

[12] Roslan, N.H., Ismail, M., Abdul-Majid, Z., Ghoreishiamiri, S., Muhammad, B. (2016): Performance of steel slag and steel sludge in concrete. *Construction and Building Materials,* 104, pp. 1–24, https://doi.org/10.1016/j.conbuildmat.2015.12.008.

[13] Penteado, C.S.G., Evangelista, B.L., dos Santos Ferreira, G.C., Borges, P.H.A., Lintz, R.C.C. (2019): Use of electric arc furnace slag for producing concrete paving blocks. *Ambiente Construído, Porto Alegre*, 19(2), pp. 21–32, http://dx.doi.org/10.1590/s1678-86212019000200305.

[14] Wang, G.C. (2016): 8 - Unbound slag aggregate use in construction. In: *The Utilization of Slag in Civil Infrastructure Construction*, Woodhead Publishing Series in Civil and Structural Engineering: Number 68, Wang, G.C. (ed.). Elsevier Ltd., SPi Global: India, pp. 155–184, https://doi.org/10.1016/B978-0-08-100381-7.00008-2.

[15] Gonawala, R.J., Kumar, R., Chauhan, K.A. (2019): Usage of Crushed EAF Slag in Granular Sub-base Layer Construction. In: *Proceedings of ICIIF 2018,* Springer Nature, Singapore, Gateway East Singapore, pp. 257–266.

[16] Skaf, M., Manso, J.M., Aragón, Á., Fuente-Alonso, J.A., Ortega-López, V. (2017): EAF slag in asphalt mixes: A brief review of its possible re-use. *Resources, Conservation and Recycling*, 120, pp. 176–185. http://dx.doi.org/10.1016/j.resconrec.2016.12.009.

[17] Maharaj, C., White, D., Maharaj, R., Morin, C. (2017): Reuse of steel slag as an aggregate to asphaltic road pavement surface. *Cogent Engineering*, 4(1), pp. 1–12, doi.org/10.1080/23311916.2017.1416889.

[18] Vaiana, R., Balzano, F., Iuele, T., Gallelli, V. (2019): Microtexture performance of EAF slags used as aggregate in asphalt mixes: A comparative study with surface properties of natural stones. *Applied Sciences*, 9(15), 3197, pp. 1–14, https://doi.org/10.3390/app9153197.

[19] Češnovar, M., Traven, K., Horvat, B., Ducman, V. (2019): The Potential of Ladle Slag and Electric Arc Furnace Slag use in Synthesizing Alkali Activated Materials; the Influence of Curing on Mechanical Properties. *Materials,* 12(7), 1173, pp. 1–18, doi:10.3390/ma12071173.

[20] Vahčič, M., Milačič, R., Mladenovič, A., Murko, S., Zuliani, T., Zupančič, M., Ščančar, J. (2008): Leachability of Cr(VI) and other metals from asphalt composites with addition of filter dust. *Waste Management*, 28, pp. 2667–2674, doi:10.1016/j.wasman.2008.01.003.

[21] Šturm, T., Milačič, R., Murko, S., Vahčič, M., Mladenovič, A., Strupi Šuput, J., Ščančar, J. (2009): The use of EAF dust in cement composites: Assessment of environmental impact. *Journal of Hazardous Materials,* 166, pp. 277–283, doi:10.1016/j.jhazmat.2008.11.015.

[22] Zalar Serjun, V., Mladenovič, A., Mirtič, B., Meden, A., Ščančar, J., Milačič, R. (2015): Recycling of ladle slag in cement composites: environmental impacts. *Waste Management*, 43, pp. 376–385, http://dx.doi.org/10.1016/j.wasman.2015.05.006.

[23] Milačič, R., Zuliani, T., Oblak, T., Mladenovič, A., Ščančar, J. (2011): Environmental impacts of asphalt mixes with electric arc furnace steel slag. *Journal of Environmental Quality*, 40, pp. 115–1161, doi:10.2134/jeq2010.0516.

[24] Wang, G.C. (2016): 7 - Environmental aspects of slag utilization. In: *The Utilization of Slag in Civil Infrastructure Construction*, Woodhead Publishing Series in Civil and Structural Engineering: Number 68, Wang, G.C. (ed.). Elsevier Ltd., SPi Global: India, pp. 131–153, https://doi.org/10.1016/B978-0-08-100381-7.00007-0.

[25] SIST EN 1744-3 (2002). *Tests for chemical properties of aggregates. Part 3, Preparation of eluents by leaching of aggregates.*

[26] SIST EN 12457-4 (2004). *Characterisation of waste – Leaching – Compliance test for leaching of granular waste materials and sludges. Part 4, One stage batch test at a liquid to solid ratio of 10 L/kg for materials with particle size below 10 mm (without or with size reduction).*

[27] Vidmar, J., Zuliani, T., Novak, P., Drinčić, A., Ščančar, J., Milačič, R. (2017): Elements in water, suspended particulate matter and sediments of the Sava River. *Journal of Soils and Sediments*, 17(7), pp. 1917–1927, doi 10.1007/s11368-016-1512-4.

[28] Decree on waste (2015): Official Gazette of Republic Slovenia RS, No. 37/15 and No. 69/15.

Original scientific paper

Received: Feb 28, 2020
Accepted: Mar 20, 2020
DOI: 10.2478/rmzmag-2020-0005

Production and Investigation of New Cast Aluminium Alloy with Lithium Addition

Izdelava in preiskava nove livarske aluminijeve zlitine z dodatkom litija

Bastri Zeka, Boštjan Markoli, Primož Mrvar, Blaž Leskovar, Mitja Petrič*
University of Ljubljana, Faculty of Natural Sciences and Engineering, Department of Materials and Metallurgy, Aškerčeva 12, 1000 Ljubljana, Slovenia
* mitja.petric@omm.ntf.uni-lj.si

Abstract
Lithium additions to Al offer the promise of substantially reducing the weight of alloys, since each 1 wt. % Li added to Al reduces density by 3 % and increases elastic modulus. In the present work, the effect of 1.46 wt. % Li addition to AlSi7Mg (containing 7.05 wt. % Si and 0.35 wt. % Mg) was studied. The alloy showed reduced density and higher hardness after natural ageing. Experimental work showed that microstructural and mechanical properties changed with Li addition. It was observed that 0.80 wt. % Li addition resulted in formation of new phase AlLiSi which has a great effect to increase hardness of AlSi7Mg. According to Scanning Electron Microscope (SEM) and X-ray diffraction analysis it was confirmed that the addition of Li causes formation of different phases which are: α-Al, β-Si and AlLiSi.

Key words: aluminium, ageing, microstructural constituents, precipitation, mechanical properties.

Povzetek
Dodatki litija (Li) aluminijevim zlitinam prispevajo k bistvenemu zmanjšanju teže zlitin, saj vsak dodani odstotek litija zmanjša gostoto za 3 %. Litij tudi povzroči povečanje elastičnega modula. V delu je preučen dodatek 1.46 mas. % litija livarski zlitini AlSi7Mg, ki vsebuje 7.05 mas. % Si in 0.35 mas.% Mg. Zlitina je pokazala zmanjšanje gostote in večjo trdoto po naravnem staranju. Rezultati so pokazali, da so se mikrostrukturne in mehanske lastnosti spreminjale z dodatkom Li. Izkazalo se je, da dodatek 0.80 mas. % Li povzroči pojav nove faze AlLiSi, ki močno vpliva na povečanje trdote AlSi7Mg. Glede na rezultate vrstične elektronske mikroskopije (SEM) rentgensko difrakcijsko analizo (XRD) je bilo potrjeno, da dodatek Li povzroči nastanek različnih faz, ki so: α-Al, β-Si in AlLiSi.

Ključne besede: aluminij, staranje, mikrostrukturne sestavine, precipitacija, mehanske lastnosti.

Introduction

Al-Li base alloys have low density, high elastic modulus and high strength properties which make these alloys attractive for aerospace applications. The high strength is produced by the process of precipitation hardening. The addition of elements can form incoherent dispersoid or semicoherent precipitates and change the microstructure and mechanical properties of alloys [1–5]. Al-Li alloys use in aircraft applications, where the weight savings effected by using these low-density alloys greatly reduce the vehicle fuel costs and increase performance of parts such as: Aircraft parts such as leading and trailing edges, access covers, seat tracks; military and space applications such as main wing box, centre fuselage, control surfaces are made by Al-Li alloys. Al-Li alloys are used as substitute for conventional aluminium alloys in helicopters, rockets and satellite systems [5–8]. The precipitates of Al-Li alloys are in several metastable and stable phases which can be present in Al-Li alloys, depending on the alloying elements. The metastable precipitates in this section are δ' (Al_3Li), while the stable phase discussed is δ (AlLi) [8]. The precipitation, in turn, depends upon chemistry, grain structure, and total thermomechanical history. In Al-Li alloys, the strengthening from Li additions is due to both solid solution strengthening and precipitation hardening [1–20]. The precipitation hardening is primarily due to the metastable strengthening phase, δ' (Al_3Li), which forms spherical, coherent, and ordered precipitate particles having a cube-on-cube orientation relationship with the aluminium matrix [20–25]. At equilibrium, and at its simplest in binary Al-Li alloys, the only phases present are the aluminium-rich solid solution and the δ (AlLi) phase [25–30].

New aluminium cast alloy was produced and analysed with Li additions based on AlSi7Mg alloy with improved mechanical properties where characterisation of solidification path was determined with all microstructural constituents. In order to develop new alloys with Li addition was used an optic microscope and Scanning electron microscopy (SEM) Thermal analysis and differential scanning calorimetry in accordance with thermodynamic equilibrium calculations were used to determine the solidification course. Also, XRD analyses and mechanical testing (hardness testing,) were performed.

Experimental Work

New aluminium cast alloy AlSi7MgLi was investigated experimentally. The thermodynamic calculations were performed with ThermoCalc software and the chemical compositions of alloys given in Table 1 were used in order to calculate phase diagrams of alloys. Samples were melted in an induction furnace in a graphite crucible and cast in a steel mould where simple thermal analysis was performed. After data acquisition their numerical data, cooling curves and their derivatives were plotted and characteristic temperatures determined. Differential scanning calorimetry was performed, and sample prepared for microstructural investigation with optic microscope and scanning electron microscope with EDS in order to determine the phases present in alloy AlSi7Mg. Vickers Hardness test was used to determine mechanical properties in period of 30 days after casting.

Table 1: *Chemical composition of alloy in wt. %.*

Alloy	Al	Si	Fe	Cu	Mg	Zn	Ti	Li
AlSi7Mg	Rest	6.7	0.44	0.01	0.35	0.01	0.01	-
AlSi7MgLi	Rest	7.05	0.10	0.05	0.36	0.02	0.09	0.80

Results and Discussion

Thermodynamic description of system AlSi7MgLi cast alloys was constructed using ThermoCalc software. From the chemical composition in Table 1 the solidification and equilibrium phases were calculated for experimental alloy. According to the thermodynamic equilibrium calculation we have predicted solidification of the primary α-Al, β-Si, new phases (AlLiSi), Mg_2Si, iron bearing phase π- AlMgFeSi and β-AlFeSi.

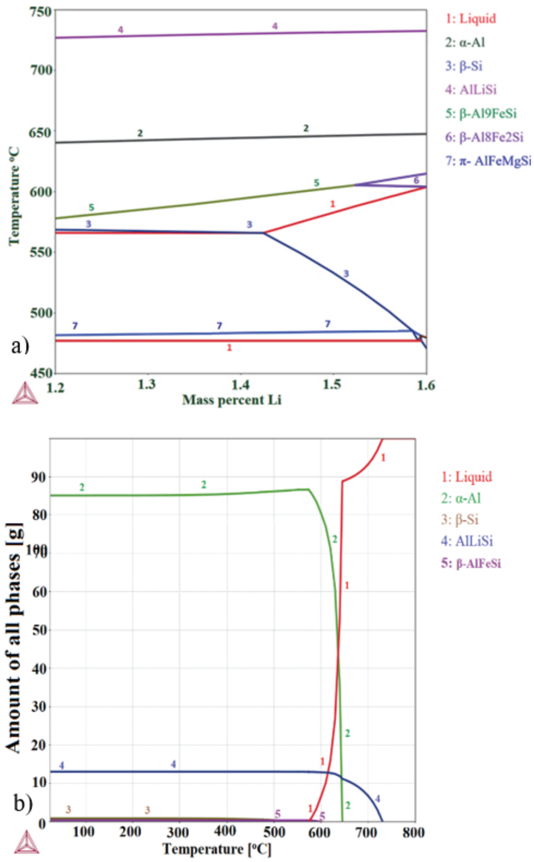

Figure 1: *a) phase diagram of experimental alloy AlSi7MgLi and b) amount of phases of alloy during solidification.*

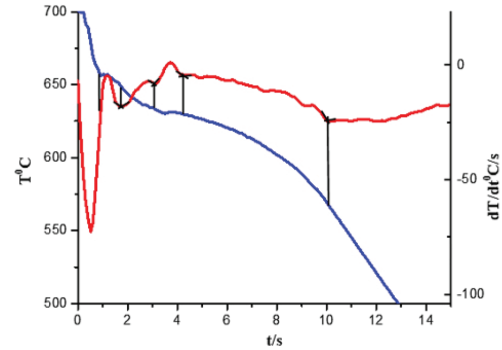

Figure 2: *The cooling curve and differentiated curves of AlSi7MgLi alloy.*

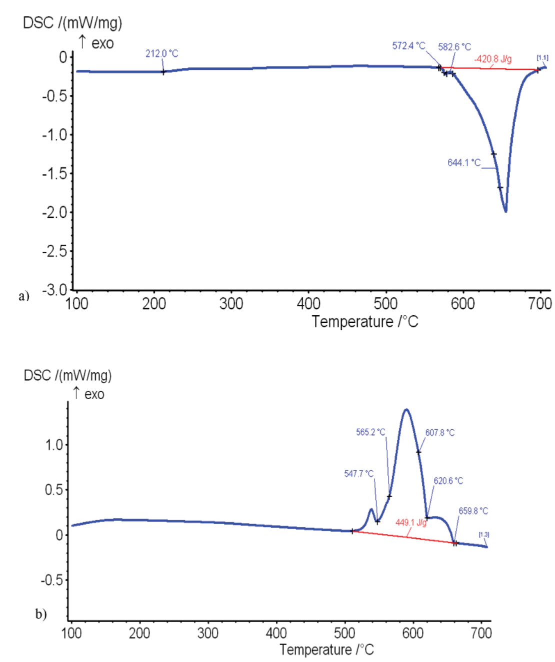

Figure 3: *Heating DSC curve (a) and cooling DSC curve (b) of AlSi7MgLi alloy.*

Thermal Analysis

Solidification process was analysed by thermal analysis on the samples cast in the steel mould and croning cell, each sample subjected to the solidification by cooling in the air. After the data acquisition their numerical and graphical processing with the marked temperatures of the phase transformations was performed. The cooling and differentiated curves of AlSi7Mg alloy with Li addition from casting temperature 730 °C in steel mould are shown in Figure 2. Diagram with cooling curves in the Figure 2 indicates interactive significant deviation in values of the characteristic temperatures of the solidification, acording to calculation and diargram of cooling curves at 730 °C with solidification start phases at 658 °C. Solidification interval ended at 570 °C.

The heating curve indicates melting start at 572 °C and the curve changes after 582.6 °C and continued with evaluation of phase at 644.1 °C, furthermore small peaks at 212 °C indicates precipitation process. Simultaneous thermal analysis was performed on the sample part from the sample poured in the steel mould, differential scanning calorimetry (DSC) resulted in diagrams of the heating and cooling curves shown in the figure 3-a and 3-b. Diagrams in the Figure 3 resulted in values of significant temperatures of the phase transformations. The temperature of the solidification start (liquidus temperature) at 659.8 °C with AlLiSi phase at 620.6 °C, the α-Al+AlLiSi should solidify according to thermocalc at 607.8 °C, followed by iron

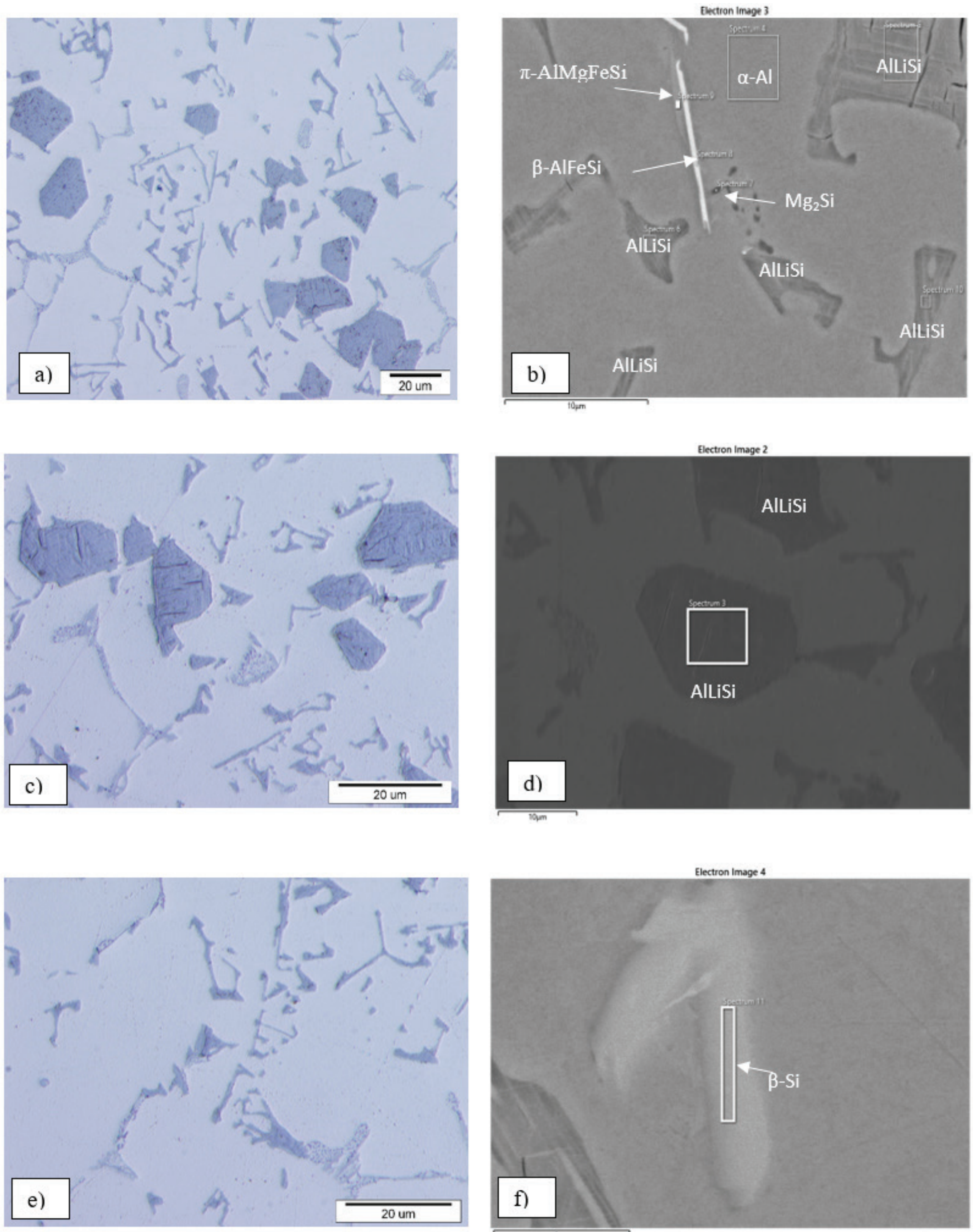

Figure 4: *Optical (a, c, e) and SEM micrographs (b, d, f) of AlSi7MgLi.*

bearing phase β-AlFeSi at 565.2 °C, β-Si and Mg_2Si at 547.7 °C.

Microstructure Analysis

After analysis of solidification by thermal analysis technique samples were prepared for metallographic investigation. According to micrographs the microstructure consists of α-Al phase, AlLiSi phase, π- AlMgFeSi phase, Mg_2Si which they are confirmed by EDS and XRD analysis and they presented in Figure 4b, 4d, 4f and Figure 5. With SEM we observed phases which

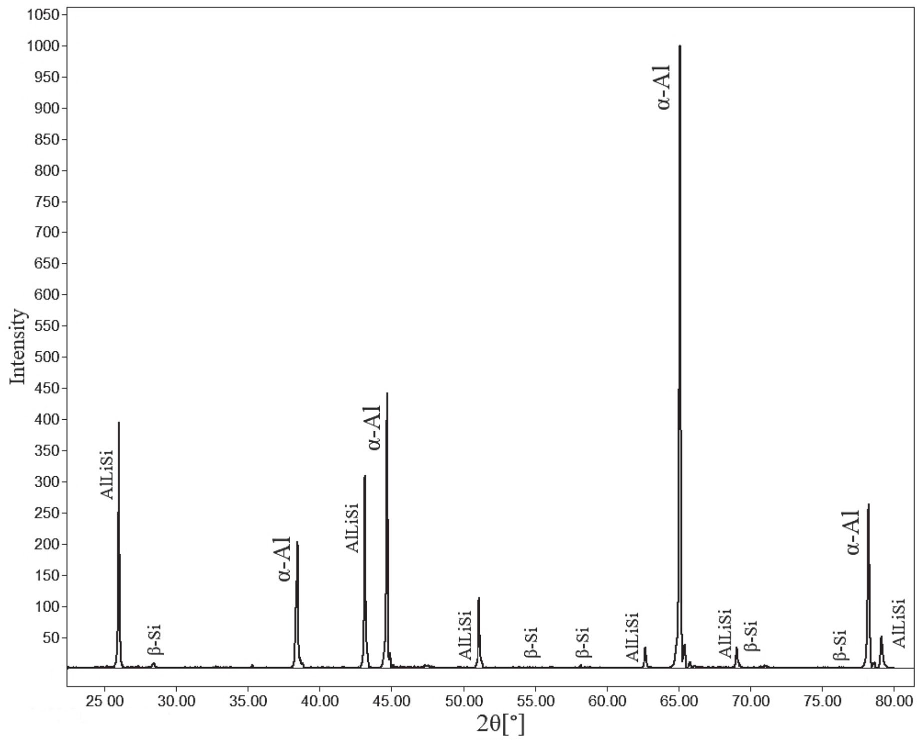

Figure 5: *XRD pattern of AlSi7MgLi alloy.*

they are formed with Li addition. From Figure 4 it can be concluded that new phase AlLiSi appears. According to thermocalc calcalucaltion the elemental composition of phase present as-cast state alloy the percentage of each element in the phase of AlLiSi is 33 wt %, after analysis by SEM- EDS it was proved that AlSi contain lithium according to the thermodynamic calculation. Furthermore, microstructure in the alloy with Li addition consists from α-Al, β-AlFeSi, π- AlMgFeSi and Mg_2Si. With XRD analysis we observed phases which they are formed with Li addition. From Figure 5 we confirm the formations of alpha α-Al, AlLiSi phases and β-Si.

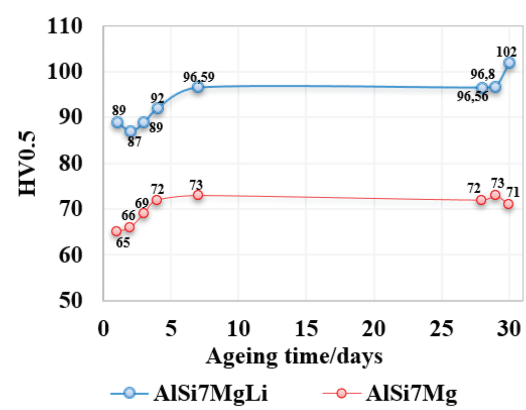

Figure 6: *presents graph of hardness for natural ageing of AlSi7Mg and AlSi7MgLi.*

Mechanical Properties

The samples were age-hardened for 30 days where 8 micro hardness measurements were performed at room temperature and average values were calculated.

Hardness test analysis for sample AlSi7Mg for first measurement was 66 HV. During 2–4 measurements, values showed a linear increase of hardness from 66 HV-73 HV. It can be concluded that peak hardness was achieved after 7 days.

Hardness test analysis for sample AlSi7MgLi showed the hardness for first day was 89 HV as cast state. After 24 hours of ageing, the hardness of sample dropped until 87 HV. After 2 to 7 days hardness of AlSi7MgLi alloy increased gradually from 87 HV to 96 HV where plateau is reached at 96 HV. It can be concluded that peak of hardness was achieved after 30 days at 102 HV. Our research showed that value of hardness increased during 30 days of ageing time from 65–73 at AlSi7Mg whereas at AlSi7Mg with Li addition from 89–102 HV. According to results of both alloys, the Li addition to AlSi7Mg has great influence on increasing of hardness compared to AlSi7Mg.

Conclusion

New alloy with Li addition to AlSi7Mg alloy was studied. For this purpose 1.46 wt. % Li was added to designed AlSi7MgLi alloy containing 0.36 wt. % Mg and 7.05 wt. % Si. It was found that Li combination with AlSi7Mg resulted on different solidification, development of new microstructure and creation of new phase AlLiSi. Li has influence to increase the mechanical properties in as cast state to AlSi7Mg. SEM/ EDS and XRD analysis revealed that the addition of Li promotes the formation of new phase α-Al, β-Si and AlLiSi.

References

[1] Prasad, E.N., Gokhale, A., Wanhill, R.J.H. (2014): *Aluminium-Lithium Alloys*. Butterworth-Heinemann: Oxford, pp. 99–103.

[2] Polmear, I., StJohn D., Nie J.F., Qian M. (2017): *Light Alloys-Metallurgy of the Light Metals*. Butterworth-Heinemann: Oxford, pp. 55–110.

[3] Brown, J.R. (1999): *Foseco non-ferrous foundryman's handbook*. Butterworth-Heinemann: Oxford, 288 p.

[4] ASM Metals Handbook, (1990): Vol 02, *Properties and Selection: Nonferrous Alloys and Special-Purpose Materials*. ASM Internationl, pp. 250–300.

[5] Polmear, I. (2006): *Light Alloys; From Traditional Alloys to Nanocrystals*. Butterworth-Heinemann: Oxford, pp. 55–150.

[6] Backerud, L., Chai G., Tamminen J. (1990): Solidification characteristics of aluminium alloys. *American Foundry Society*, pp. 52–80.

[7] Polmear, I.J., Ringer, S.P. (2000): Evolution and control of microstructure in aged aluminium alloys. *Journal of Japan Institute of Light Metals,* 50, pp. 633–642.

[8] Polmear, IJ. (1999): Control of precipitation processes and properties in aged aluminium alloys by microalloying. *Materials Forum*, pp. 23–117.

[9] Baker, C., Gregson P.J., Harris, S.J., Peel, C.J. (1986): Aluminium-Lithium Alloys III. In: *Proceedings 3rd International Conference on Aluminum-Lithium Alloys*. The Institute of Metals: London, UK, pp. 509–515.

[10] Bagaryatsky, Y.A. (1952): Deformation behaviour of the AlMg4.5Cu0.5 type alloy sheet. *Dokl Akad*., 87, pp. 559–562.

[11] Adam, C.M. (1981): *Aluminium-Lithium Alloys.* AIME, New York: NY, pp. 37–48.

[12] Anyalebechi, P.N. (1995): Analysis of the effects of alloying elements on hydrogen solubility inliquid aluminum alloys. *Scripta Metallurgica Materialla*, 33(8), pp. 1209–1216.

[13] Ashton, R.F., Thompson, D.S., Starke Jr., E.A., Lin, F.S. (1986): Processing Al-Li-Cu-(Mg) alloys. In: *Aluminium-Lithium Alloys III.,* Baker, C., Gregson, P.J., Harris, S.J., Peel, C.J. (eds.). The Institute of Metals: London, UK, pp. 66–77.

[14] Averill, W.A., Olsen, D.L., Matlock, D.K., Edwards, G.R. (1981): Lithium reactivity and containment. In: *Proceedings of the First International Aluminium-Lithium Conference*, Sanders, T.H., Starke, E.A. (eds.). The Metallurgical Society of AIME: Warrandale, PA, pp. 9–28.

[15] Binczeveki, G. (1986): Producing aluminium-lithium ingot encased in outer metal cladding. *Light Met.*, Age June, pp. 31–36.

[16] Birch, M.E.J. (1986): Grain refining of aluminium-lithium based alloys with titanium boron aluminium. In: *Aluminium-Lithium Alloys III*, Baker, C., Gregson, P.J., Harris, S.J., Peel, C.J (eds.). The Institute of Metals: London, UK, pp. 152–158.

[17] Birch, M.E.J., Cowell, A.J. (1987): Titanium-carbon-aluminium: a novel grain refiner for aluminium-lithium alloys. In: *Proceedings of the Fourth International Conference on Aluminium-Lithium Alloys*, Champier, G., Dubost, B., Miannay, D., Sabetay, L. (eds.). J. Phys., Colloque, 48 (C3), p. 108.

[18] Bretz, P.E. (1987): Alithalites alloy development and production. In: *Proceedings of the Fourth International Conference on Aluminium-Lithium Alloys*, Champier, G., Dubost, B., Miannay, D., Sabetay, L. (eds.). J. Phys, pp. 25–31.

[19] Bretz, P.E., Gilliland, R.G. (1987): The intensive development programme that produced aluminium-lithium alloys. *Light Met.,* Age April, pp. 5–12.

[20] Cassada, W.A., Shiflet, G.J., Starke, E.A. (1986): The effect of Germanium on the precipitation and deformation behaviour of Al-2Li alloys. *Acta Metallurgica*, 34(3), pp. 367–378.

[21] Chakravorty, C.R., Singh, V., Gokhale, A.A. (1987): Melting and casting of aluminium-lithium alloys. In: *Proceedings of the 36th Annual Convention of Institute of Indian Foundrymen (IIF),* The Institute of Indian Foundrymen: Calcutta, India, pp. 135–140.

[22] Colvin, G.N., Tak, J.H., Veeck, S.J. (1988): An investment cast Al-Li alloy *HTC 321*. In: *Aluminium-Lithium Alloys: Design, Development and Application Update*, Kar, R.J., Agarwal, S.P., Quist, W.E. (eds.). ASM International: Metals Park, OH, pp. 453–465.

[23] De Ross, A.B., Mondolfo, L.F. (1980): Metallurgical aspects of casting aluminium alloys. In: *Aluminium Transformation Technology*, Pampilo, C.A., Biloni, H., Embury, D.E. (eds.). ASM: Metals Park, OH, pp. 81–140.

[24] Dinsdale, K., Harris, S.J., Noble, B. (1981): Relationship between microstructure and mechanical properties of aluminium-lithium-magnesium alloys. In: *Aluminium-Lithium Alloys, Proceedings of the First International Aluminium-Lithium Conference*, Sanders, T.H., Starke, E.A. (eds.). The Metallurgical Society of AIME: Warrendale, PA, pp. 101–118.

[25] Divecha, A.P., Karmarkar, S.D. (1981): Casting problems specific to aluminium-lithium alloys. In: *Aluminium-Lithium Alloys I*, Sanders, T.H., Starke, E.A. (eds.). AIME: New York, NY, pp. 49–62.

[26] Divecha, A.P., Karmarkar, S.D. (1986): The search for aluminium-lithium alloys. *Advanced Materials & Processes Incorporating Metal Progress*, 10, pp. 75–79.

[27] Fedosov, A.S., Danilkin, V.A., Grigoryeva, A.A. (1992): Influence of lithium on balance between hydrogen and aluminium melts. *Tsvetn. Met. 2, 61–63. Foote Mineral Co. Bulletin, 1984.* Technical Data Bulletin, p. 101.

[28] Fridlyander, I.N., Bratukhin, A.G., Davydov, V.G. (1992): Soviet Al-Li alloys of aerospace application. In: *'Aluminium-Lithium', Volume 2, Conf. Proc. Sixth. International Aluminium-Lithium Conference, 1991*, Peters, M., Winkler, P.J. (eds.). DGM Information gesellschaft, Verlag: Germany, pp. 35–42.

Original scientific paper

Received: Jan 31, 2020
Accepted: Mar 19, 2020
DOI: 10.2478/rmzmag-2020-0004

Engineering Site Investigation and Shallow Foundation Design in Ore Area of Ondo State, Nigeria

Inženirsko kartiranje in načrtovanje plitvega temeljenja na območju Ore v zvezni državi Ondo, Nigerija

Olumuyiwa, O. Falowo
Department of Civil Engineering Technology, Faculty of Engineering Technology, Rufus Giwa Polytechnic, Owo, Ondo State, Nigeria
oluwanifemi.adeboye@yahoo.com

Abstract

The study integrates geophysical and geotechnical methods for subsoil evaluation and shallow foundation design. The study involved six vertical electrical sounding and geotechnical investigation involving cone penetration test and laboratory soil analysis. Three major geologic units were delineated; the topsoil, weathered layer and partly weathered/fractured/fresh bedrock. The overburden thickness is in between 15.2–32.9 m. Based on resistivity (16–890 ohm-m) and thickness (12.7–32 m) the weathered layer is competent to distribute structural load to underlying soil/rock. The groundwater level varies from 4.5 to 12.3 m. Therefore an average allowable bearing capacity of 200 kPa is recommended and would be appropriate for design of shallow foundation in the area, at a depth not less than 1.0 m with an expected settlement ranging from 9.03–48.20 mm. The ultimate bearing and allowable bearing capacity for depth levels of 1–3 m vary from 1403–2666 kPa and 468–889 kPa for strip footing while square footing varies in between 1956–3489 kPa and 652–1163 kPa respectively.

Key words: cone penetration test, vertical electrical sounding, settlement analysis, bearing capacity, Ore southwestern.

Povzetek

Raziskava se ukvarja z geofizikalnimi in geotehničnimi metodami za ocenjevanje plasti pod površjem in z načrtovanjem plitvega temeljenja. V raziskavo je bilo vključenih šest navpičnih električnih sondiranj in geotehničnih preiskav, kot so preizkus s statičnim konusnim penetrometerom (CPT) in laboratorijske preiskave zemljin. Razmejene so bile tri glavne geološke enote; zgornja plast tal, preperela plast in delno preperela/razpokana/sveža podlaga. Debelina nadkritja je med 15.2–32.9 m. Na osnovi upornosti (16–890 ohm-m) in debeline (12.7–32 m) je preperela plast ustrezna za prenos konstrukcijske obtežbe na nižje ležečo zemljino/kamnino. Gladina podtalnice niha med 4.5 do 12.3 m pod površjem. Zato je priporočena povprečna dovoljena nosilnost 200 kPa, ki bi bila primerna za načrtovanje plitvega temeljenja na tem območju, z globino ne manj kot 1.0 m in s pričakovanim posedanjem v območju med 9.03–48.20 mm. Mejne in dovoljene nosilnosti pasovnih temeljev za globine 1–3 m so 1403–2666 kPa in 468–889 kPa, za kvadratne temelje pa 1956–3489 kPa in 625–1163 kPa.

Ključne besede: preizkus s statičnim konusnim penetrometrom, navpično električno sondiranje, analiza posedkov, nosilnost tal, JZ Ore.

Introduction

Shallow Foundations are usually located no more than six feet below the lowest finished floor [1–3]. A shallow foundation system generally used when the soil close the ground surface has sufficient bearing capacity, and underlying weaker strata do not result in undue settlement. The shallow foundations are commonly used most economical foundation systems. Footings are structural elements, which transfer loads to the soil from columns, walls or lateral loads from earth retaining structures. In order to transfer these loads properly to the soil, footings must be design to: prevent excessive settlement; minimize differential settlement; and provide adequate safety against overturning and sliding. Deep foundations are usually used when the conditions of the upper soil layers are weak and unable to support the superstructure loads [4]. Piles carry these superstructure loads deep in the ground. Therefore, the safety and stability of pile supported structures depend on the behavior of piles [5–6]. Most soil deposits in Ore are soft in nature.

There are different methods commonly used in assessing the in-situ geo-mechanical properties of the soil; the use of geophysical techniques, such as electrical resistivity method (VES) or seismic method; direct probing using static or dynamic penetration techniques and or boreholes. The success in the applicability of geophysical techniques depends on so many factors. The most important one is that there must be significant and detectable contrast between the physical properties of the different units in the subsurface, such as velocity, electrical resistivity, conductivity, density, acoustic properties, subsurface geology and the environmental conditions. Among these techniques, electrical resistivity method has a lots of applications: evaluation of temperature of soil and water content, evaluation of soil salinity, groundwater and mining survey and geotechnical investigation and geological mapping [7–9]. In addition, the 1D electrical method had been improved to a two dimensional imaging of the subsurface [10–11]. More recently, D-C electrical resistivity methods had been used for environmental studies [12] soil characterization for engineering purposes [13] and mapping of growth fault. In addition cone penetration test (CPT) is considered the most frequently used method for characterization of geomedia [14–16]. The CPT is basically advancing a cylindrical rod with a cone tip into the soil and measuring the tip resistance and sleeve friction due to this intrusion. The resistance parameters are used to classify soil strata and to estimate strength and deformation characteristics of soils. The CPT is a simple, quick, and economical test that provides reliable in situ continuous soundings of subsurface soil [17–19]. Due to the soft nature of soil deposits in Ore, Ondo State, Nigeria the CPT is considered a perfect perfect tool for the area's site characterization. In subsurface exploration, the CPT in conjunction with SPT or in correlation with laboratory analysis of samples have effectively used to identify and classify soils and to evaluate the undrained shear strength. Implementation of the CPT can drastically decrease the number of soil borings and reduce the cost and time required for subsurface characterization. Following the standardization of test procedure [20] and improvement on the method of data interpretation [21], its reliability is found to be excellent. Mechanical cone, electric cone, and piezocone are the devices commonly used in cone penetration testing. The mechanical type is least efficient and least sensitive to changes in soil conditions, sensitive to changes in soil conditions. The goals of this research is to identify and estimate the bearing capacity of the subsoil layering through geophysical, cone penetration test data, and laboratory sampling analysis, for design of foundation and bases [22] in the study area.

Material and Methods

Description of the Study Area

The study area is Odigbo Local Government of Ondo State. The area can access through Akure – Ore Lagos – Benin highways and is located within latitude 715000–75500 mN and longitude 664750–725000 mE (Figure 1). Major part of the study area is devoted to agricultural and commercial activities. The study area falls within the tropical rainforest climate. The average temperature is 25 °C. Relative humidity of the area differs within 70% to 80%. The av-

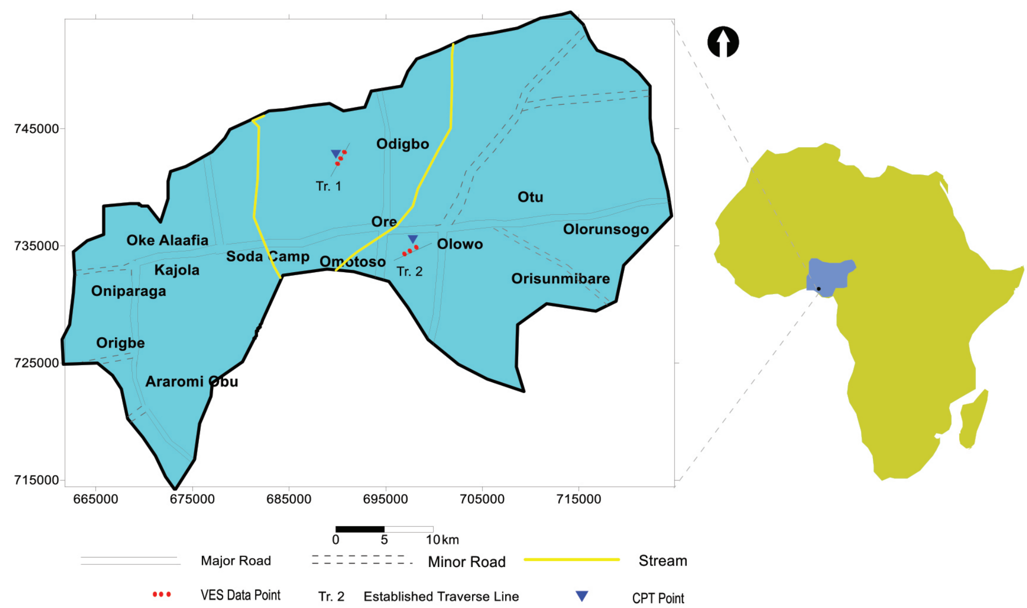

Figure 1: *Location Map showing data acquisition points.*

erage annual rainfall of the study area is about 1500 mm and 2500 mm [23]. The topographic elevation ranges from 110–185 m. The northern area falls within the geologic terrain, underlain by the Precambrian basement complex rocks of southwestern Nigeria, characterized by the migmatite-gneiss complex, older granites, charnockites, quartzite and minor intrusive lithologies [24–25]. The local geology consists of charnockite, fine grained biotite granite and gneiss in the north (Figures 2 and 3). Field observation shows that biotite granites in the area occur as large igneous bodies, and largely coarse grained. However the southern parts of the study area is underlain by Coastal plain sands of Benin formation; Ewekoro and Akinbo; and Abeokuta formations (Figure 2).

The Abeokuta Formation in surface outcrops comprises mainly sand with sandstone, siltstone, silt, clay, mudstone and shale interbeds. It usually has a basal conglomerate which may measure about 1 m in thickness and generally consists of poorly rounded quartz pebbles with a silicified and ferruginous sandstone matrix or a soft gritty white clay matrix. In outcrops where there is no conglomerate, coarse, poorly sorted pebbly sandstone with abundant white clay constitutes the basal bed. The overlying sands are coarse grained, clayey, micaceous and poorly sorted, and indicative of short distances of transportation or short duration of weathering and possible derivation from the granitic rocks located to the north. The Ewekoro Formation overlies the Araromi Formation in the eastern Dahomey basin (Figure 2). It is an extensive limestone body, which is traceable over a distance of about 320 km from Ghana in the west, towards the eastern margin of the Dahomey basin in Nigeria. Okosun [26] has reported that the limestone is of shallow marine origin owing to abundance of coralline algae, gastropods, pelecypods, echinoid fragments and other skeletal debris. It is Paleocene in age. Overlying the Ewekoro Formation is the Akinbo Formation, which is made up of shale and clayey sequence [27]. The claystones are concretionary and are predominantly Kaolinite. The base of the Formation is defined by the presence of glauconitic band with lenses of limestone [26–27]. The Formation is Palaeocene to Eocene in age. The area is well drained by rivers and streams that flow in the same direction as the rock strike. These streams take their source from relatively high elevation about 200 m above the mean sea level and flow downhill along the strike into valleys.

Data Collection and Analysis

Subsurface investigations employing geophysical techniques are of paramount importance in assessing the suitability of an area for the con-

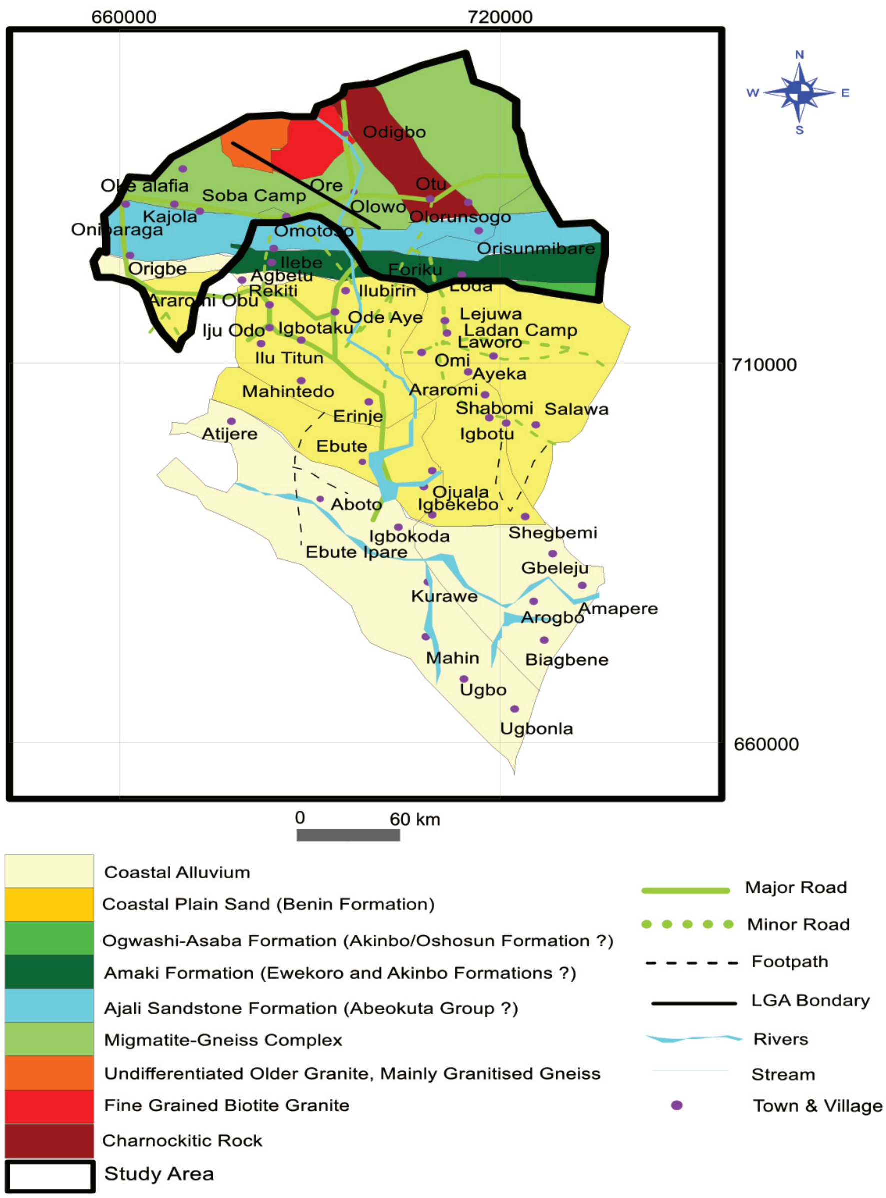

Figure 2: *Geological map of Southern part of Ondo State.*

struction of buildings, roads, bridges, etc. The method has been proven to be an effective tool for identifying anomalies and defining the complexity of the subsurface geology [10–28]. The electrical imaging or electrical tomography is a survey technique recently developed for the investigation of areas of complex geology. Electrical resistivity imaging was carried out along two established traverses in N - S direction and six VES were conducted in order to delineate the resistivity of the subsurface materials. The technique was used so as to delineate the overburden, weathered zones, fractured columns and where possible, the bedrock at the site. Six (06) Schlumberger vertical electrical soundings (VES) were conducted across the study area using a maximum current electrode separation (AB) of 100 m. Figure 1 shows the VES locations. Resistivity measurements were made with a digital resistivity meter (Ohmega) which allows for readout of current (I) and voltage (V). The field curves were interpreted through partial curve matching with the help of master curves and auxiliary point charts

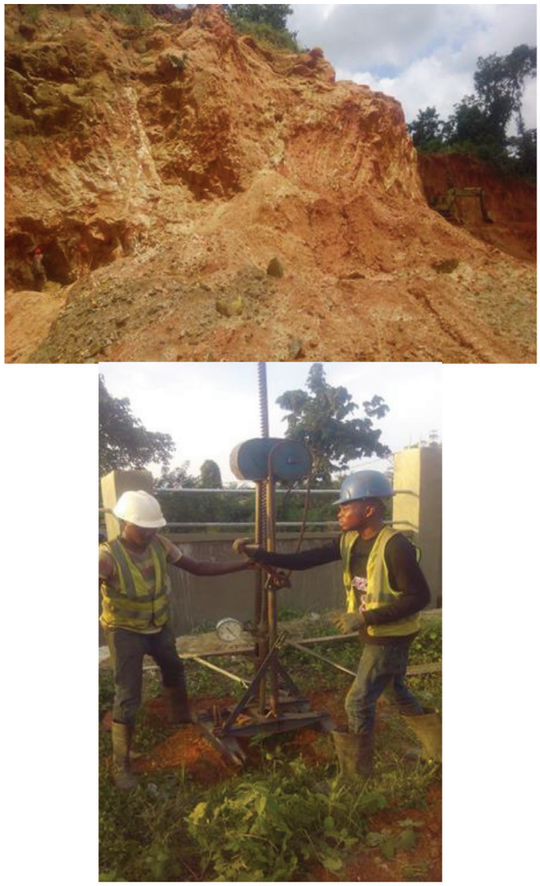

Figure 3: *Field Pictures of the thick lateritic clay deposit in Odigbo and Cone penetration test.*

[29–30]. From the preliminary interpretation, initial estimates of the resistivity and thickness of the various geoelectric layers at each VES location were obtained. These geoelectric parameters were later used as starting model for a fast computer-assisted interpretation [31–32]. The program takes the manually derived parameter as a starting geoelectric model, successively improved on it until the error is minimized to an acceptable level. Cone penetration test**s** were performed at a total of six (6) locations within the study area (Figure 1). The tests were carried out to a depth of 3 m. The Dutch static penetration measures the resistance of penetration into soils using a 60 ° steel cone with an area of 10.2 cm^2.

The cone penetrometer test is a means of ascertaining the resistance of the soil. The layer sequences are interpreted from the variation of the values of the cone resistance with depth. The test is carried out by securing the winch frame to the ground by means of anchors. These anchors provided the necessary power to push the cone into the ground. The cone and the tube are pushed together into the ground for 20 to 25 cm; the cone is pushed ahead of the tube for 3.5 cm at a uniform rate of about 2 cm/sec [33–34]. The resistance to the penetration of the cone registered on the pressure gauge connected to the pressure capsule is recorded. The tube is then pushed down and the procedure described above repeated. From the series of recorded gauge readings, cone resistance and sleeve friction are plotted against depth.

The layer sequences were interpreted from the variation of the values of the cone resistance with depth. The allowable bearing pressure of the soil layers on each location was calculated using Meyerhof [35] and Schmertmann [36] equation direct method for estimating ultimate bearing capacity (q_{ult}) from cone resistance for square and strip footings, as shown in equations (1) to (5):

$$q_{ult} = q_c \left(\frac{B}{12.2}\right)\left(1 + \frac{D_f}{B}\right) \quad (1)$$

q_c = cone resistance value
D_f = Depth of footing
B = Width of foundation

Factor of safety at least 3 is recommended by Meyerhof to obtain the allowable bearing pressure.

For cohensionless soils:

Strip $q_{ult} = [(28 - 0.0052\,(300 - q_c)^{1.5}]98$ kPa (2)

Square $q_{ult} = [(48 - 0.0052\,(300 - q_c)^{1.5}]98$ kPa (3)

For clay:

Strip $q_{ult} = (2 + 0.28q_c)\,98$ kPa (4)

Square $q_{ult} = (5 + 0.34q_c)\,98$ Kpa (5)

All samples obtained in the field were carefully preserved and subjected to more detailed visual inspection and descriptions at the laboratory. Thereafter, representative samples were selected from each stratum for laboratory analysis in accordance with relevant geotechnical engineering standards including BS 1377 [37]. The disturbed soil samples were appropriately subjected to the following laboratory classification tests: natural moisture content; Atterberg limits (liquid and plastic limits); grain size analysis; and unconsolidated undrained triaxial tests at different cell pressures. Sieve analysis of cohesive soils were done by soaking oven-dried samples in water overnight and washing through sieve No. 200 (75 microns opening) while remnants retained on sieve No. 200 were oven-dried and sieved mechanically. Materials finer than sieve number 200 were analyzed using the hydrometer method based on Stoke's Law. Total consolidation settlement (s) has been computed for foundation breadth (B) between 0.5–3.0 m, subjected to an allowable bearing capacity of 100 kPa. The induced vertical stress ($\Delta\sigma$) at the centre of the consolidating layer has been used in computing s. The final consolidation settlement has been computed from the expression below [38] using Equation (6):

$$s = m_v H \Delta\sigma' \qquad (6)$$

m_v = coefficient of volume compressibility
H = thickness of compressible layer
$\Delta\sigma'$ = average increase in effective pressure which was varied from 0.02–0.16MPa

An average m_v value of 0.125 m^2/KN which corresponds to the adopted net allowable bearing capacity, was used in the settlement analysis and also corresponds to stiff clay (with compression index of 0.15 to 0.06), although this was based on the result of the laboratory experiment performed on the soil samples within the study area. The value of m_v adopted also corresponds to the range given by [39] of 0.25–0.125 m^2/KN. Coefficient of volume compressibility (m_v) is more useful parameter than coefficient of permeability, because for a particular soil m_v is not constant but depends on the pressure range considered.

Results and Discussion

The VES curves identified in the area are H, QH, and KH types with three to four geoelectric layer combinations. The QH curve type predominates, constituting 50% of the total, the KH curve type constitutes 33.3% and H curve type constitute 16.7%. The geoelectric section along Traverse 1 in Odigbo (Figure 4) identified maximum of four geoelectric/geologic subsurface layers comprising the topsoil, weathered layer, partly weathered/fractured basement/fresh basement. The topsoil varies in composition from clay to clayey sand, sandy clay and lateritic clay with resistivity values ranges from 68 to 689 ohm-m and thickness varies from 0.9–2.5 m. The resistivity of this layer has average of 200 ohm-m whose geoelectric characteristic is typical of sandy clay. The weathered layer resistivities are generally within the range of 46 and 890 ohm-m, typical of clay, clayey sand, and laterite. Resistivity in the range of 40–200 ohm-m is the most dominant, signifying a clayey weathered layer, The thickness is moderately thick with values varying from 12.7 m to 20.5 m and generally. The partly weathered/fractured basement/fresh basement has layer resistivity values vary from 882–1464 ohm-m. The depth to (overburden thickness) this layer is in between 15.2–22.1 m. Information gathered from existing hand dug well and boreholes shows that the groundwater level varies from 7.4 to 9.5 m. Therefore the weathered layer could be stabilized prior construction to improve the geotechnical properties since it's predominantly clayey. This would reduce consolidation settlement usually associated with clay. The thickness of the topsoil is very thin to accommodate civil engineering foundation structure because the upper 1 m is usually removed during construction to guide against undue settlement arising from buried/decayed plants and animals. The groundwater level ranges between 4.5–6.2 m.

Along Traverse 2 in Ore metropolis, the geoelectric section (Figure 5) also delineates maximum of four geoelectric/geologic subsurface layers comprising the topsoil, weathered layer, partly weathered/fractured basement/fresh basement. The topsoil has resistivity values ranging from 69 to 228 ohm-m and thickness

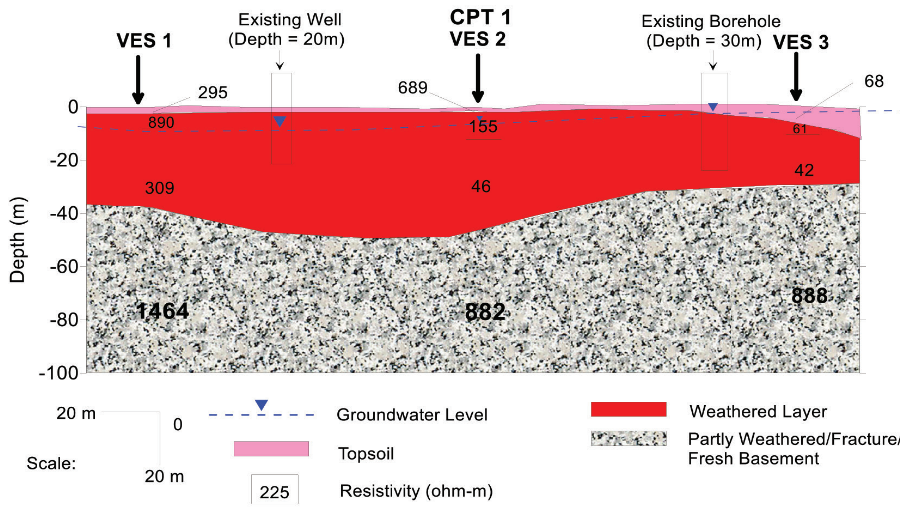

Figure 4: *Geoelectric Section along Traverse 1 in Odigbo.*

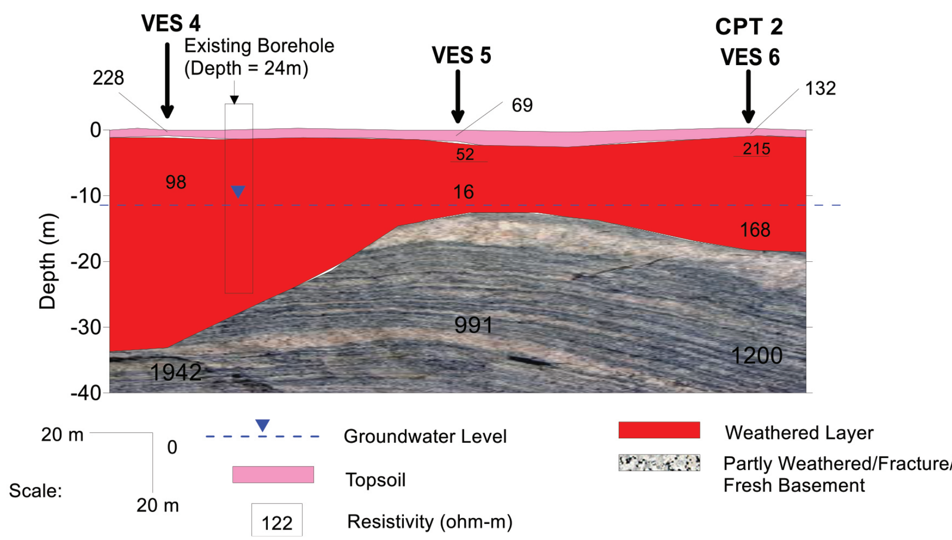

Figure 5: *Geoelectric Section along Traverse 2 in Ore.*

varies from 0.9– 2.0 m. It varies in composition from clay to clayey sand. The weathered layer resistivities are generally within the range of 16 and 215 ohm-m, typical of clayey soil. The thickness is moderately thick with values varying from 17.5 to 32 m. The partly weathered/ fractured basement/fresh basement has layer resistivity values vary from 991–1200 ohm-m. This is the major aquifer in the area especially where the fracture basement is extensive with high fracture density/lineament interception. The depth to (overburden thickness) this layer is in between 19.5–32.9 m. The groundwater level measured from an existing well along this Traverse under VES 4/VES 5 records 12.3 m. Consequently this water level may not pose any/serious threat to foundation structure in the area. Therefore the weathered layer thickness is thick enough to distribute structural load to underlying soil/basement rock. But appreciable degree of stabilization (especially mechanical stabilization) to improve the geotechnical properties since it's predominantly clayey. This would also reduce consolidation settlement usually associated with clay soil material.

Table 1: *Geotechnical/Engineering Properties of soil in location 1.*

Depth (m)	Cone Resistance	Sleeve Resistance	Friction Ratio	L.L (%)	P.L (%)	P.I (%)	S.L (%)	M.C (%)	% Gravel	% Sand	% Silt	% Clay	S.G
0.2	20	35	1.75	30.5	20.3	10.2	9.9	6.3	0.1	25.3	56.9	17.7	2.65
0.4	40	60	1.50										
0.6	58	70	1.21	27.2	19.4	7.80	6.3	10.5	0.2	44.6	43.5	11.7	2.65
0.8	50	60	1.20										
1.0	62	70	1.13	35.8	20.9	14.9	10.2	12.6	-	22.0	54.9	22.8	2.65
1.2	70	90	1.29										
1.4	85	120	1.41	34.1	19.8	14.3	11.8	12.2	-	28.4	63.3	8.4	2.65

Table 2: *Geotechnical/Engineering Properties of soil in location 2.*

Depth (m)	Cone Resistance	Sleeve Resistance	Friction Ratio	L.L (%)	P.L (%)	P.I (%)	S.L (%)	M.C (%)	% Gravel	% Sand	% Silt	% Clay	S.G
0.2	20	30	1.50	41.6	24.1	17.53	7.9	11.8	-	32.0	31.2	36.8	2.70
0.4	35	50	1.43										
0.6	50	70	1.40	51.7	30.1	21.61	9.1	18.7	-	43.6	20.8	35.6	2.69
0.8	60	85	1.42										
1.0	60	90	1.50	57.3	37.4	19.93	8.6	16.8	-	36.9	28.9	34.1	2.69
1.2	100	140	1.40										

The summary of the geotechnical results is shown in Tables 1 and 2.

The % gravel ranges from 0.1–0.2, sand varies in between 22–44.6%, % silt varies from 20.8–63.3, and clay ranges from 8.4–36.8%. Generally the soil is dominated by sandy silt (SM). The average clay content in the soil is less than 35% which falls within 35% recommended for subsoil material that are good for civil engineering foundation construction. The specific gravity of the soil recorded values in the range of 2.65 (sand)–2.70 (clay). The average percentage passing 0.075 m is 33.3% which falls within 35% recommended for subsoil material that are good for construction. The engineering parameters of the soil samples are within the federal ministry of works and housing [40] specification for civil engineering building foundation construction. The analyzed soil samples at both locations shows liquid limits of 27.2–57.3% (avg. 39.7%), plastic limits of 19.4–37.4% (avg. 24.57%), plasticity index of 7.80–21.61% (avg. 15.18%) and shrinkage limits of 6.3–11.3% (avg. 9.1%) indicating moderate soil quality [41–42]. Generally, the lower the linear shrinkage, the lesser the tendency for the soil to shrink when desiccated [41–42]. The natural moisture content ranges from 6.3–18.7% (avg. 12.7%) which is moderately low. The FMWH [40] recommends liquid limit of 50% maximum, plastic limit of 30% maximum, plastic index of 20% maximum and 8% maximum for foundation material. Hence, the soil can be adjudged as a good foundation soil.

The results of cone resistance with depth shows increase in cone resistance and sleeve resistance with depth (Tables 1 and 2), range from 20–85 kg/cm^2 and 35–120 kg/cm^2 at CPT 1, and 20–100 kg/cm^2 and 30–140 kg/cm^2 at CPT 2 respectively. The friction ratio ranges from 1.13–1.75 (CPT 1) and 1.40–1.50 (CPT 2). The Robertson [43] soil chart classification (Figure 6) shows two dominant zones of 6 to 7 corresponding to sandy silt to clayey silt and silty

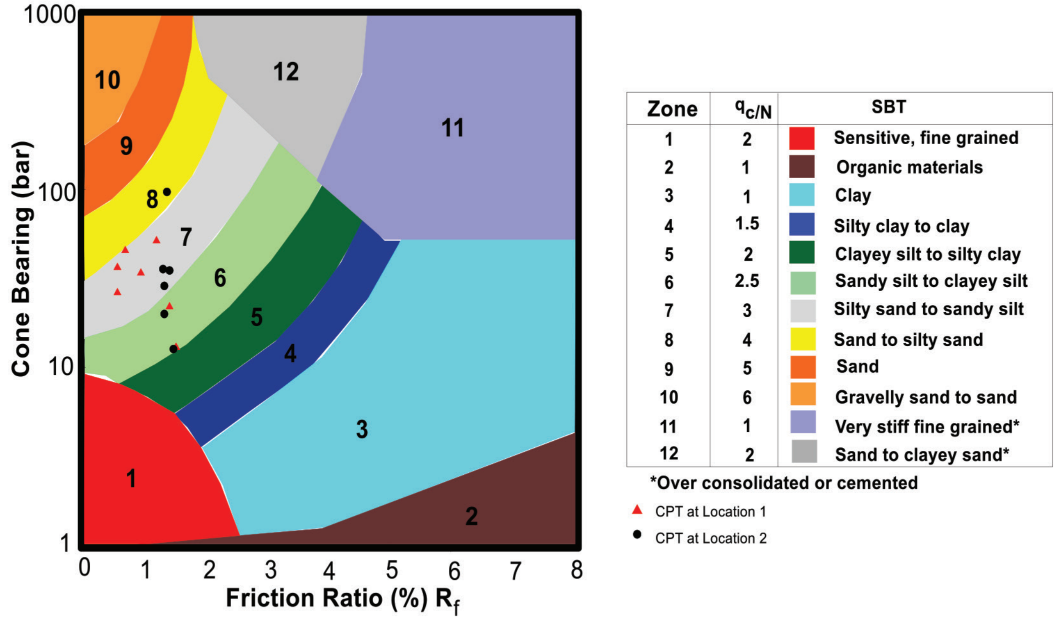

Figure 6: *Robertson Chart for the soil classification using cone resistance and friction ratio values.*

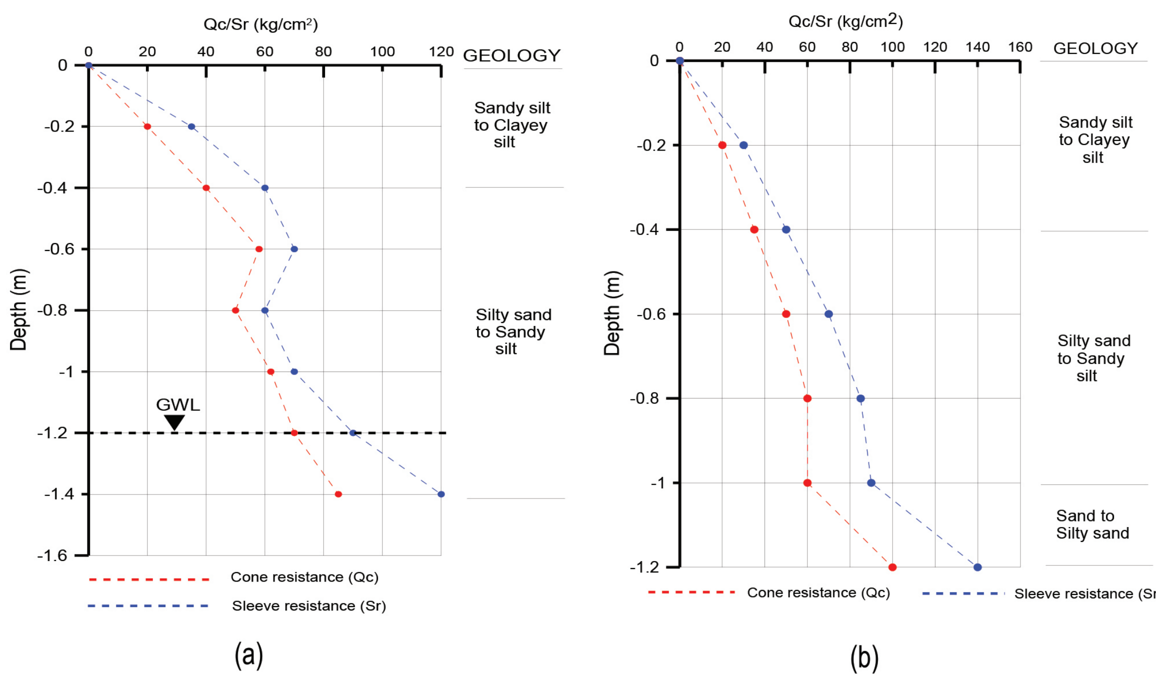

Figure 7: *Plots of Cone resistance and sleeve resistance against depth at location 1 and 2, corresponding to (a) Odigbo CPT 1 (b) Ore CPT 2.*

sand to sandy silt respectively (Figure 7). The plots of cone resistance and sleeve resistance against depth (Figure 8) showed two geological succession of sandy silt to clayey silt (0–0.4 m) and silty sand to sandy silt (0.4–1.4 m) at CPT 1 and three geologic sequence in CPT 2, namely sandy silt to clayey silt (0–0.4 m), and silty sand to sandy silt (0.4–1.0 m). Consequently, at least depth of 1.0 m would be appropriate as found-

Table 3: *Bearing Capacities estimated from the Cone resistance values for both sites (locations).*

Depth (m)	CPT 1		CPT 2	
	(kPa)	(kPa)	(kPa)	(kPa)
0.2	49	147	49	147
0.4	98	294	86	257
0.6	142	426	123	368
0.8	123	368	147	441
1.0	152	456	147	441
1.2	172	515	245	735
1.4	208	625	-	-

Table 4: *Settlement variation at Different Depths and Foundation Widths.*

Foundation width (m)	Settlement (mm) at Depth Level (m)		
	1 m	2 m	3 m
0.6	43.97	45.64	48.20
1.2	24.49	27.20	30.70
1.5	20.13	23.07	26.82
2.0	14.53	17.54	21.33
3.0	9.03	12.32	16.21

Table 5: *Bearing Capacities for Strip and Square Shallow Foundations in the Study area.*

Depth (m)	Strip	Square	Strip	Square
	(kPa)	(kPa)	(kPa)	(kPa)
1	1403	1956	468	652
2	1870	2523	623	841
3	2666	3489	889	1163

ing depth for design and construction of shallow foundation in the area.

The ultimate and allowable bearing capacity estimated from the cone resistance using Meyerhof [35] equation are presented in Table 3. The calculated bearing capacities could be used in determining the foundation type for structures. The allowable bearing of the soil varies between 49 to 208 kPa for CPT 1, and 49–245 kPa for CPT 2 and ultimate bearing capacity of 147 to 625 kPa and 147 to 735 kPa respectively. Consequently an average allowable bearing capacity of 200 kPa (ultimate bearing capacity of 600 kPa) is recommended and would be appropriate for design of shallow foundation in the area, at a depth not less than 1.0 m in location 1 and 1.4 m at location 2.

Settlement and bearing capacity are the major factors that govern foundation design. The commonly accepted basis of design is that the total settlement of a footing should be restricted to about 25 mm [34], [42–44] as by so doing the differential settlement between adjacent footings is confined within limits that can be tolerated by a structure. The settlement analysis for foundation width of 0.6–3.0 m at three depth levels of 1 m, 2 m and 3 m produces values between 30.06–45.92 mm (Table 4). But foundation width above 1.5 m produces settlement less than 25 mm (Table 5) recommended by Bell [42] as it ranges between 9.03–21.33 mm. Although according to Meyerhof [35], Schmertamnn [36] total settlement limits of 60 mm (clay) and 50 mm (granular soil) are still tolerable [45]. Therefore foundation width not less than 1.5 m for depth not less than 0.6 m is still feasible and appropriate. The calculation of bearing capacities for strip and square foundation is shown in Table 5. For strip foundation, the appropriate (recommended) ultimate bearing and allowable bearing capacity for depth levels of 1–3 m vary from 1403–2666 kPa and 468–889 kPa, while square footing varies in between 1956–3489 kPa and 652–1163 kPa respectively (Table 6).

Conclusion

Subsoil evaluation and shallow foundation design have been carried out in Ore area of Ondo State, Nigeria for civil engineering structure using geophysical and geotechnical method of investigations. The investigation was able to provide information on the stratigraphy, nature, structural disposition, competence of the subsoil. It also recommended appropriate foundation bearing capacities and corresponding expected settlements for different footing sizes and founding depths. The VES curves identified in the area are H, QH, and KH types with three to four geoelectric layer combinations. The QH curve type predominates, constituting 50% of the total, the KH curve type constitutes 33.3% and H curve type constitute 16.7%. The investigation delineated four geologic layers which include the topsoil, weathered layer, partially weathered/fractured basement/fresh bedrock. The groundwater level measured from an existing well and borehole ranged from 4.5–12.3 m. Consequently this water level may not pose any/serious threat to foundation structure in the area. Therefore the weathered layer thickness is thick enough to distribute structural load to underlying soil/basement rock. But appreciable degree of stabilization (especially mechanical stabilization) to improve the geotechnical properties since it's predominantly clayey. This would also reduce consolidation settlement usually associated with clay soil material. All the determined geotechnical parameters of the subsoil fall within the specification recommended for foundation material by FMWH. In view of this, an average allowable bearing capacity of 200 kPa (ultimate bearing capacity of 600 kPa) is recommended and would be appropriate for design of shallow foundation in the area, at a depth not less than 1.0 m in location 1 and 1.4 m at location 2. This would produce settlement values ranging from 9.03–48.20 mm depending on the width of the foundation. The ultimate bearing and allowable bearing capacity for depth levels of 1–3 m vary from 1403–2666 kPa and 468–889 kPa for strip footing while square footing varies in between 1956–3489 kPa and 652–1163 kPa respectively.

References

[1] Das, B.M. (1983): *Advanced soil mechanics*. Hemisphere Publishing Corporation: Washington, DC, 51 p.

[2] Teng, W.C. (1962): *Foundation Design*. Prentice-Hall International, Inc.: Englewood Cliffs, N.J., 119 p.

[3] Peck, R.B., Hanson, W.E., Thornburn, T.H. (1953): *Foundation Engineering.* John Wiley & Sons, Inc.: New York, 243 p.

[4] Terzaghi, K., Peck, R.B. (1967): *Soil Mechanics in Engineering Practice,* 2nd edition. John Wiley & Sons, Inc.: New York, 491 p.

[5] Garg, S.K. (2009): *Soil mechanics and foundation engineering*, 7th revised edition. Khanna Publishers: New Delhi, 752 p.

[6] Vesic, A.S. (1963): *Bearing capacity of deep foundation in sand*. Highway Research Method. No. 39, pp. 112–153.

[7] Olorunfemi, M.O., Idonigie, A.I., Coker A.T., Babadiya, G.E. (2004): The Application of the Electrical Resistivity Method in Foundation Failure Investigation. A Case Study of O.A.U. Ile-Ife, Dental Clinic. *Global Journal of Geophysical Science,* 2(1), pp. 139–151.

[8] Oyedele, K.F., Olorode, D.O. (2010): On Site Investigation of Subsurface Conditions using Electrical Resistivity Method and Cone Penetration Test at 'Medina Brook Estate, Gbagada, Lagos, Nigeria. *World Applied Science Journal*, 11(9), pp. 1097–1104.

[9] Oyedele, K.F., Bankole, O.O. (2009): Subsurface Stratigraphic Mapping using Geophysics and its impact in urbanization in Arepo area, Ogun State, Nigeria. *New York Science Journal*, (5)2, pp. 31–45.

[10] Loke, M.H., Barker, R.D. (1996): Rapid least-squares inversion of apparent resistivity pseudosections by a quasi-Newton method. *Geophysical Prospect*ing 44, pp. 131–152.

[11] Badmus, B.S., Akinyemi, O.D., Olowofela, J.A., Folarin, G.M. (2012): 3D electrical resistivity tomography survey for the basement of the Abeokuta terrain of Southwestern Nigeria. *J. Geol. Soc. India*, 80, p. 845, DOI: 10.1007/s12594-012-0213-x.

[12] Sharma, P.V. (1997): *Environmental and Engineering Geophysics*. Cambridge University Press, p. 173.

[13] Olayanju, G.M., Mogaji, K.A., Lim, H.S., Ojo, T.S. (2017): Foundation integrity assessment using integrated geophysical and geotechnical techniques: case study in crystalline basement complex, southwestern Nigeria. *Journal of Geophysics and Eng*ineering 14(3), pp. 675–690.

[14] ISOPT-1. (1988): Cone penetration test. International reference test procedure. In: *Proceedings of the First International Symposium on Penetrating Testing, ISOPT-1*, Orlando California, de Ruiter, J. (ed.). A.A. Balkema: Rotterdam; Brookfield.

[15] Huijzer, G.P. (1990): Automated stratigraphic classification of CPT data. In: *Proceedings 6th International Congress IAEG*, Amsterdam, Price, D.G (ed.). A.A. Balkema: Rotterdam; Brookfield, pp. 309–311.

[16] Juang, C.H., Huang, X.H., Holtz, R.D., Chen, J.W. (1996): Determining relative density of sands from CPT using fuzzy sets. *Journal of Geotechnical Engineering*, 122(1).

[17] Harder, H., Von, B.V. (1988): Determination of representative CPT parameters. Penetration testing in the UK. In: *Proceedings of the Geotechnology Conference*, Birmingham, Telford, T. (ed.). London, pp 237–240.

[18] Broms, B.B. (1986): Penetration tests. In: *Proceedings of the 4th International Geotechnical Seminar*, Singapore. Nanyang Technological Institute: Singapore.

[19] Biddle, D.W. (1989): Penetration testing in the UK. In: *Proceedings of the Geotechnology Conference*, Birmingham, Telford, T. (ed.). London, pp 189–191.

[20] Owuama, C.O. (2000): A comprehensive method of interpretation of static cone data. *NSE Technical Transactions*, 35(1), pp. 53–66.

[21] Lunne, T., Robertson, P.K., Powell, J.J.M. (1997): *Cone Penetration Testing in Geotechnical Practice*. Blackie Academic and Professional: London, 312 p.

[22] Schmertmann, J. H. (1970): Static Cone to Compute Static Settlement over Sand. *Journal of the Soil Mechanics and Foundations Division*, 96(SM3), pp. 1011–1043.

[23] Iloeje, M.P. (1981): *A new Geography of Nigeria*. Longman: Nigeria, pp. 26–28.

[24] Rahaman, M.A. (1982): Review of the Basement Geology of Southwestern Nigeria. In: *Geology of Nigeria*, Kogbe C.A. (ed.). Elizabethan Pub. Co.: Lagos, pp. 41–58.

[25] Jones, H.A., Hockey, R.D. (1964): The geology of part of Southwestern Nigeria. *Geological Survey of Nigeria*, Bull. 31, p. 87.

[26] Okosun, E.A. (1998): Review of the Early Stratigraphy of Southwestern Nigeria. *Journal of Mining and Geology,* 34(1), pp. 27–35.

[27] Omatsola, M.E., Adegoke, O.S. (1981): Tectonic evolution and cretaceous stratigraphy of the Dahomey Basin. *Nigerian Journal of Mining and Geology*, 18(1), pp. 130–137.

[28] Zhdanov, M.S., Keller, G.V. (1994): *The Geoelectrical methods in geophysical exploration*. Elsevier: Amsterdam, 873 p.

[29] Keller, G.V., Frischknecht, F.C. (1966): *Electrical Methods in Geophysical Prospecting*. Pergamon Press: Oxford, 519 p.

[30] Telford, W.M., Geldart, L.P., Sheriff, R.E. (1990): *Applied Geophysics*, 2nd edition. Cambridge University Press: Cambridge, 792 p.

[31] Sirles, P. (2006): Advancement in 3D Subsurface Modelling using Seismic Refraction Data- A new perspective. In: *Proceedings for GEOPHYSICS 2006, 3rd International Conference on Applied Geophysics*, St. Louis MO.

[32] Cosenza, P., Marmet, E., Rejiba, F., Cui, Y.J., Tabbagh, A., Charlery, Y. (2006): Correlations between geotechnical and electrical data: a case study at Garchy in France. *Journal of Applied Geophysics*, 60, pp. 165–178.

[33] Robertson, P.K., Campanella, R.G. (1983): Interpretation of cone penetration test part 1 sand. *Canadian Geotechnical Journal*, 30(4), pp. 734 –745.

[34] Mazlan, A. (2007): *Correlation between Cone Penetration Test and Bearing Capacity for Shallow Foundation*. Master's Thesis. Universiti Teknologi Malaysia.

[35] Meyerhof, G.G. (1976): Bearing capacity and settlement of pile foundations. *ASCE Journal of the Geotechnical* Engineering, 12(GT3), pp.194–228.

[36] Schmertmann, J.H. (1978): *Guidelines for Cone Penetration Test, Performance and Design*. U.S. De-

partment of Transportation, Report No. FHWA-TS-78–209, Washington, D.C., p.145.

[37] British Standard Institutions (1990): *Methods of Test for soils for Civil Engineering Purposes*. B.S 1377: Part 2, 1990, pp. 8–200.

[38] Stroud, M.A., Butler, F.G. (1975): The standard penetration test and the engineering properties of Glacial materials. In: *Proceedings of the Symposium of glacial materials*, University of Birmingham.

[39] Upadhyay, A.K. (2015): *Soil and Foundation Engineering*, Second Edition. S.K. Kataria & Sons: New Delhi, 245 p.

[40] Federal Ministry of Works and Housing (1972): *Highway Manual Part 1 Road Design*, Federal Ministry of Works and Housing: Lagos.

[41] Jegede, G. (2000): Effect of soil properties on pavement failure along the F209 highway at Ado-Ekiti, Southwestern Nigeria. *Journal of Construction and Building Materials*, 14, pp. 311–315.

[42] Bell, F.G. (2007): *Engineering Geology*. Elsevier, 352 p.

[43] Robertson, P.K. (1990): Soil classification using the cone penetration test. *Canadian Geotechnical Journal,* 27, pp. 151–158.

[44] Vesic, A.S. (1967): Ultimate loads and settlement of deep foundations in sand. In: *Proc. Symp. bearing capacity and settlement of foundations*. Duke University, pp 53–68.

[45] Eslami, A., Gholami, M. (2002): Bearing capacity of shallow foundations from CPT data. In: P*roceeding of 3rd Iranian International Conference on Geotechnical Engineering and Soil Mechanics*, pp. 93–97.

Original scientific paper

Received: Jan 07, 2020
Accepted: Feb 11, 2020
DOI: 10.2478/rmzmag-2020-0001

The Deposition Temperature Dependence on the Crystallite Size of NiO Thin Films

Said Benramache[1,*], Foued Chabane[2], Ali Arif[3]

[1] Department of Material Sciences, University of Biskra, Biskra 07000, Algeria
[2] Department of Mechanical, University of Biskra, Biskra 07000, Algeria
[3] Department of Electrical, University of Biskra, Biskra 07000, Algeria
* s.benramache@univ-biskra.dz

Abstract

In this article, we have investigated a fitting proposal model for calculating the crystallite size of pure NiO thin films by varying the structural parameters, such as full width at half-maximum β, lattice parameter a and differences in $a - a_0$. The experimental data of NiO thin films were prepared at several deposition temperatures in the range of 380–460°C. All estimated values of crystallite sizes are proportional to the experimental data. Thus, the measurement of the crystallite size values by this proposed model is compatible with practical measurements qualitative.

Keywords: NiO thin films, deposition temperature, crystallite size, defect structure, fitting.

Povzetek

V tem delu smo preučili skladnost modela za izračun velikosti kristalnih zrn v tankih plasteh čistega NiO s spreminjanjem strukturnih parametrov, kot so FWHM β, mrežni parameter a in razlika v $a - a_0$. Eksperimentalni podatki, pridobljeni iz tankih plasti NiO uporabljeni v modelu so bili pripravljeni pri različnih temperaturah nanosa v območju od 380 do 460°C. Ocene velikosti kristalnih zrn so skladne z eksperimentalnimi podatki. Na osnovi tega, je meritev velikosti kristalnega zrna po predlaganem modelu skladna s praktičnimi meritvami in predstavlja kvalitativnimi rezultat.

Ključne besede: tanke plasti NiO, temperatura nanosa, velikost kristalnega zrna, strukturne napake, ujemanje

Introduction

In previous years, the investigation of new materials for photovoltaic applications was dependent and related to the experimental and modelling parameters of any properties. Nickel oxide was obtained to belong in the group of semiconductor materials and is one of the best materials at present because of its good properties [1].
Nickel oxide (NiO) is a semiconductor material with a nature of p-type, which belonged to the part of TCO family. This attribute of NiO has several potential applications, for example, it is used in the gas sensors due to its band gap energy in the range of 3.6–4.0 eV and for the organic solar cells applications due to its p-type semiconducting [2]. It can be used in transparent diodes and even in the transparent transistors caused by the best optical transmission and electrical conductivity. Moreover, NiO can be used for defrosting windows due to its good conductivity, and fabricated NiO can be used in the UV photodetectors and touch screens due to its good responsivity [3, 4].
In the present article, we have studied and investigated a relationship to calculate the crystallite size (G) from the measured structural parameters of the X-ray diffraction in the NiO thin films. We have used the experimental data of NiO thin films prepared at several deposition temperatures in the range of 380–460°C [5], which present the following parameters, such as the diffraction angle 2θ, the full width at half-maximum (FWHM), the crystallite size G, the lattice parameter a and $a - a_0$ of (111) diffraction peak for NiO thin films at several deposition temperatures.

Materials and Methods

The NiO samples were fabricated on the glass substrates using a pneumatic spray technique with 0.1 M of the precursor molarity. The NiO thin films were deposited at several deposition temperatures in the range of 380–460°C [5] (see Table 1).
Table 1 presents that the NiO thin films were nanocrystalline and had a cubic structure with (111) crystal plane at the higher intensity, which has preferential a-axis orientation along with (111) crystal plane.
The Miller indices (hkl) were obtained from the Bragg equation [6]:

$$n\lambda = 2d_{hkl}\, sin\, \theta \tag{1}$$

where n, λ, d_{hkl} and θ are the integers called the order of diffraction, the wavelength longer of X-ray (λ = 1.5406 A°), the interplanar spacing and the diffraction angle, respectively.
The lattice parameter a of cubic structure for NiO thin films was determined in Eq. (1) and XRD patterns using the following formula [5]:

$$d_{h\,k\,l} = \frac{a}{\sqrt{h+k+l}} \tag{2}$$

The differences $a - a_0$ of (111) crystal plane are given by the following relation [6]:

$$a - a_0 = d_{hkl}\sqrt{h+k+l} \tag{3}$$

Table 1. *The diffraction angle 2θ, the full width at half-maximum (FWHM), the crystallite size G, the lattice parameter a and $a - a_0$ of (111) diffraction peak for NiO thin films at several deposition temperatures [5].*

Deposition temperature Ts (°C)	2θ (deg)	β (rad)	G (nm)	a (nm)	$a - a_0$ (nm)
380	37.80	0.00766	19.13	0.4122281	0.00537184
400	37.67	0.00781	18.74	0.4135872	0.00401271
420	37.64	0.00868	16.88	0.4138530	0.00374695
440	37.60	0.00799	18.31	0.4143484	0.00325152
460	37.66	0.00707	20.72	0.4136507	0.00394921

Table 2. *The crystallite size G experimental and correlated at several deposition temperatures.*

Deposition temperature Ts (°C)	Experimental crystallite size (nm)	Fitting crystallite size (nm)
380	19.13	19.14
400	18.74	18.84
420	16.88	16.96
440	18.31	18.45
460	20.72	20.82

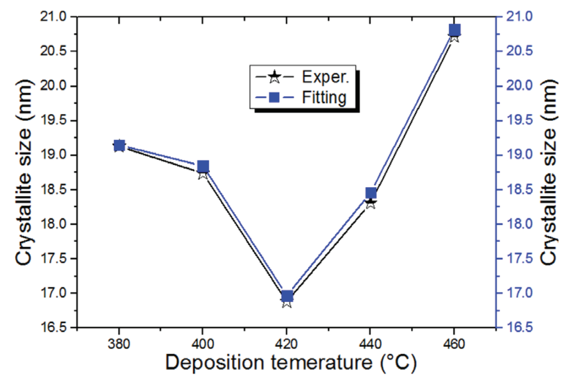

Figure 1. *The variation of the crystallite size G experimental and fitting at several deposition temperatures.*

where a_0 is the standard lattice parameter of NiO (standard a_0 = 0.4176 nm). The crystallite size of (111) crystal plane for the fabricated NiO thin films was calculated from the Scherer's formula [7]:

$$G = \frac{0.9\lambda}{\beta \cos\theta} \tag{4}$$

where G is the experiment crystallite size, β is the FWHM and θ is the diffraction angle peak (see Table 1).

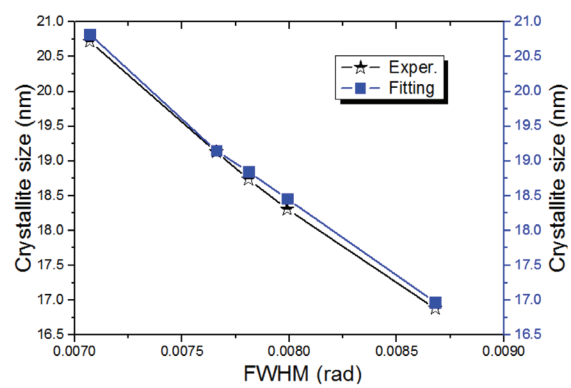

Figure 2. *The variation of the crystallite size G experimental and fitting at several FWHM values.*

Results and Discussion

In this article, we have estimated the crystallite size (G) by fitting relationships between the structural parameters (β, a and $a - a_0$), which is detected in the following empirical relationship:

$$G = C_1 \frac{a}{\beta} - C_2 \frac{a - a_0}{\beta} \tag{5}$$

where C_1 and C_2 are constants as C_1 = 0.365 and C_2 = 0.02. The results of this fitting are given in Table 2.
Figure 1 shows the variation of the experimental and fitting of the crystallite size at several deposition temperatures in the range of 380–460°C. The measured values of the crystallite sizes were obtained using Eq. (5), which were given in Table 2. This correlation indicated that the crystallite sizes of the NiO thin films can be predominantly influenced by the FWHM β, the lattice parameter a and the differences in $a - a_0$ of the NiO thin films. As seen, all estimated values of crystallite sizes are proportional to the experimental data. Thus, the measurement of the crystallite size values by this proposed model is compatible with practical measurements qualitative. This attribution can be observed with the variation of FWHM β (see Figure 2). This observation was investigated to demonstrate that the calculation of the crystallite size can be influenced by the measurements of the structural parameters (β, a and $a - a_0$).

Conclusions

In this article, the direct correlation of the crystallite size from the experimental values was investigated by a fitting model wherein the calculated crystallite size of the pure NiO thin films was detected in the structural parameters, such as the FWHM β, the lattice parameter a and the differences in $a - a_0$. The experiment data of NiO thin films were prepared at several deposition temperatures in the range of 380–460°C. All estimated values of crystallite sizes are proportional to the experimental data. Thus, the measurement of the crystallite size values by this proposed model is compatible with practical measurements qualitative.

References

[1] Diha, A., Benramache, S., Benhaoua, B. (2018): Transparent nanostructured Co doped NiO thin films deposited by sol–gel technique. *Optik*, 172, pp. 832–839.

[2] Lamastra, F.R., Nanni, F., Menchini, F., Nunziante, P., Grilli, M.L. (2016): Transparent nanostructured electrodes: Electrospun NiO nanofibers/NiO films. *Thin Solid Films*, 601, pp. 54–58.

[3] Hotovy, I., Spiess, L., Predanocy, M., Rehacek, V., Racko, J. (2014): Sputtered nanocrystalline NiO thin films for very low ethanol detection. *Vacuum*, 107, pp. 129–131.

[4] Ali, N., Hussain, A., Ahmed, R., Wang, M.K., Zhao, C., Haq, B.Ul., Fu, Y.Q. (2016): Advances in nanostructured thin film materials for solar cell applications. *Renewable and Sustainable Energy Reviews*, 59, pp. 726–737.

[5] Charef, A., Benramache, S., Aoun, Y., Benhaoua, B., Lakel, S., Marrakchi, M. (2019): Effect of Substrate Temperature on the Growth and Properties of Nanocrystalline NiO Thin Films. *Journal of Nanoelectronics and Optoelectronics*, 14, pp. 1667–1671.

[6] Aoun, Y., Marrakchi, M., Benramache, S., Benhaoua, B., Lakel, S., Charef, A. (2018): Preparation and Characterizations of Monocrystalline Na Doped NiO Thin Films. *Materials Research*, 21(2), pp. 1–5.

[7] Sharma, R., Acharya, A.D., Shrivastava, S.B., Patidar, M.M., Gangrade, M., Shripathi, T., Ganesan, V. (2016): Studies on the structure optical and electrical properties of Zn-doped NiO thin films grown by spray pyrolysis. *Optik*, 127(11), pp. 4661–4668.

Instructions for Authors

About the Journal

RMZ – Materials and Geoenvironment (RMZ – Materiali in geookolje) is a periodical publication with four issues per year. It was established in 1952 and renamed to RMZ – M&G in 1998). The main topics of Journal are Mining, Geotechnology, Metallurgy, Materials, Geology and Geoenvironment.
RMZ – M&G publishes original scientific papers, review papers, preliminary notes and professional papers in English. Only professional papers will exceptionally be published in Slovene. In addition, evaluations of other publications (books, monographs, etc.), in memoriam, presentation of a scientific or a professional event, short communications, professional remarks and reviews published in RMZ – M&G can be written in English or Slovene. These contributions should be short and clear.

- *Original scientific papers* represent unpublished results of original research.
- *Review papers* summarize previously published scientific, research and/or expertise articles on a new scientific level and can contain other cited sources which are not mainly the result of the author(s).
- *Preliminary notes* represent preliminary research findings, which should be published rapidly (up to 7 pages).
- *Professional papers* are the result of technological research achievements, application research results and information on achievements in practice and industry.
- *Publication notes* contain the author's opinion on newly published books, monographs, textbooks, etc. (up to 2 pages). A figure of the cover page is expected, as well as a short citation of basic data.
- *In memoriam* (up to 2 pages), a photo is expected.
- *Discussion of papers* (Comments) where only professional disagreements of the articles published in previous issue of RMZ – M&G can be discussed. Normally the source author(s) reply to the remarks in the same issue.
- *Event notes* in which descriptions of an scientific or a professional event are given (up to 2 pages).

Form of the Manuscript

Basic Requirements for Manuscript

- Optimal number of pages is 7 to 15; longer articles should be discussed with the Editor-in-Chief prior to submission.
- Text of the manuscript should be written in Times New Roman font with 12-point size and 1.5 line spacing.
- Figures, tables and formulas should be included in the text of the manuscript.
- Headings should be written in Arial bold font (12-point size) and should not be numbered.
- Subheadings should be written in Arial italic font (12-point size).
- The electronic version of the manuscript should be simple, without complex formatting. For highlighting, only bold and italic types should be used.
- The manuscript should be submitted in Microsoft Word via the online system.

Composition of the Manuscript

The manuscript should have the following composition:

Title

The title of the article should be precise, informative and not longer than 100 characters. The author should also indicate the short version of the title. The title should be written in English and for Slovenian authors also in Slovene.

Author's Information
Author's information should include name and surname of the authors, the address of the institution and the e-mail address of the corresponding author.

Abstract
An Abstract presents the purpose of the article and the main results and conclusions. It should not exceed 180 words. It should be written in English and for Slovenian authors also in Slovene.

Keywords
A list of up to 5 key words (3 to 5) that will be useful for indexing or searching. They should be written in English and for Slovenian authors also in Slovene.

Introduction
An Introduction should provide a review of recent literature and sufficient background information to allow the results of the article to be understood and evaluated.

Materials and methods
The Materials and method section details the theoretical or experimental methods and materials used to obtain the results.

Results and discussion
The result section should clearly and concisely present the data, using figures and tables where appropriate. The Discussion section should describe the relationships shown by results and discuss the significance of the results, making comparison with previously published work.

Conclusions
A Conclusions section should present one or more conclusions that have been made from the results and discussion.

Acknowledgements
Acknowledgement (optional) of collaboration or preparation assistance may be included. If the research was funded, please note the source of funding.

References
A references section includes a list of references, which comprises all the references cited in the text.

Units and Abbreviations

Only standard SI symbols and abbreviations should be used in the text, tables and figures. Symbols for physical quantities in the text should be written in italics (e.g. *m*, *l*, *v*, *T*). Symbols for units that consist of letters should be in plain text with spaces after number (e.g. 10 m, 5.2 kg/s, 2 s^{-1}, 50 kPa). All abbreviations should be spelt out in full on first appearance. A period/full stop is used as the decimal point (3.14 and not 3,14).

Figures

Figures must be cited in consecutive numerical order in the text and referred to in both the text and the captions as Figure 1, Figure 2, etc. Figures should be originals, made in an electronic form (Microsoft Excel, Adobe Illustrator, Inkscape, AutoCAD, CorelDraw, etc.) and saved in .eps, .tiff or .jpg format with a resolution of at least 300 dpi. The width of the figures should be at least 152 mm. Figures should be named the same as in the article (Figure 1, Figure 2, etc.). Letters and numbers should be readable, with equal sizes and fonts in all figures.
Figures should also be submitted as a separate document, i.e. separated from the text in the article.

Tables

Tables must be cited in consecutive numerical order in the text and referred to in both the text and the caption as Table 1, Table 2, etc. Tables should be prepared using a table editor and not inserted as a graphic.

Equations

Equations should be numbered in consecutive numerical order with the use of round brackets on its right side and referred in the text as Equation (1), Equation (2), etc. The equations should be written using equation editor.

References

The references should be cited in the same order as they appear in the article. Where possible the DOI for the reference should be included at the end of the reference. They should be numbered in square brackets. Any references cited in the article must be given in full. Unpublished results and personal communications are not recommended in the reference list, but may be mentioned in the text, if necessary. Please use examples in Appendix as a guide.

Manuscript Submission

Please submit your article via RMZ – M&G Editorial Manager System. You can find it on the address
http://edmgr.editool.com/rmzmag/default.htm
Log in as an author and submit your article. Note that the manuscript should be submitted in Microsoft Word format. High resolution figures should be included in the text and also submitted as a separate document.
You can follow the status of your submission in the Editorial Manager System and your e-mail.

Review Process

All manuscripts will be supervised in a review process. The reviewers evaluate the manuscript and can ask the authors to change particular segments, and propose to the Editor-in-Chief the acceptability of the submitted articles. Authors are requested to identify three reviewers and may also exclude specific individuals from reviewing their manuscript. The Editor-in-Chief has the right to choose other reviewers. The name of the reviewer remains anonymous. The technical corrections will also be done and the authors can be asked to correct the missing items. The final decision on the publication of the manuscript is made by the Editor-in-Chief.

Production Process

After composing PDF document and language editing, author receive document for proofreading. If author have any comments, mark them and write a comment in the same PDF document. Comments in another document or scanned and corrected document are inappropriate. Upload PDF document in Editorial Manager System under the different name.

If author do not cooperate in production process, manuscript can be rejected, despite of receiving letter of acceptance.

Appendix: citing of references

Journal article:

Surname 1, Initials, Surname 2, Initials (year): Title. *Journal*, volume(number), page range, DOI code. Journal title should be complete and not abbreviated. Note that *Journal Title* is italicized.

[1] Malej, S., Terčelj, M., Peruš, I., Kugler, G. (2016): Influence of cooling mode in relation to casting and extrusion parameters on mechanical properties of AA6082. *Materials and Geoenvironment*, 64(1), pp. 11–19, DOI:10.1515/rmzmag-2016-0022.

Book:

Surname 1, Initials, Surname 2, Initials (year): *Title*. Publisher: place of publication, number of pages. Note that the *Title of the book* is italicized.

[2] Reynolds, J.M. (2011): *An introduction to applied and environmental geophysics*. Wiley-Blackwell: Chichester, 710 p.

Chapter in an Edited Book:

Surname 1, Initials, Surname 2, Initials (year): Chapter title. In: *Book title*, Editor Surname 1, Initials, Editor Surname 2, Initials (ed(s).). Publisher: place of publication, page range. Note that the *Book title* is italicized.

[3] Blindow, N., Eisenburger, D., Illich, B., Petzold, H., Richer, T. (2007): Ground Penetrating Radar. In: *Environmental Geology – Handbook of Field Methods and Case Studies, Knödel*, K., Lange, G., Voigt, H.J. (eds.). Springer: Berlin, pp. 283–335.

Proceeding Paper:

Surname 1, Initials, Surname 2, Initials (year): Paper title. In: *Proceedings title*, place of symposium/conference, Editor Surname 1, Initials, Editor Surname 2, Initials (ed(s).). Publisher: place of publication, page range. Note that the *Proceedings title* is italicized.

[4] Benac, Č., Gržančić, Ž., Šišić, S., Ružić, I. (2008): Submerged Karst Phenomena in the Kvarner Area. In: *Proceedings of the 5th International ProGEO Symposium on Conversation of the Geological Heritage*, Rab, Croatia, Marjanac, T. (ed.). Pro GEO Croatia: Zagreb, pp. 12–13.

Master Thesis or Ph. D. Thesis:

Surname, Initials (year): *Title*. Type of document (Master Thesis or Ph. D. Thesis). Publisher: place of publication, number of pages. Note that the *Title* is italicized.

[5] Rošer, J. (2010): *Study of the effects of sediments on seismic ground motion in the city of Ljubljana using the microtremor survey method*. Ph. D. Thesis. University of Ljubljana, Faculty of Natural Sciences and Engineering, Department of Geotechnology, Mining and Environment: Ljubljana, 278 p.

Standard:

Standard-Code (year). *Title of the Standard*. Organisation: place. Note that the *Title of the Standard* is italicized.

[6] ISO/ICS 17892-10:2018. *Geotechnical investigation and testing – Laboratory testing of soils – Part 10: Direct shear tests*. International Organization for Standardization: Genova.

Electronic source:

Title [online]. Surname, Initials or Company name, renewed (date) [cited (date)]. Available on: *http://address*. Note that the *www address* is italicized.

[7] CASREACT – Chemical reactions database [online]. Chemical Abstracts Service, renewed 2/15/2000 [cited 2/25/2000]. Available on: *http://www.cas.org/casreact.html*.

These instructions are valid from February 2020.

ISSN 1408-7073